

Fluctuation spectra in weakly coupled Van Vleck paramagnets: Some theoretical and experimental aspects*

D. Davidov,[†] V. Zevin, R. Levin, and D. Shaltiel

Racah Institute of Physics, The Hebrew University of Jerusalem, Israel

K. Baberschke

Fachbereich Physik, Freie Universitat, Berlin, West Germany

(Received 19 January 1976)

The ESR relaxation of impurities in rare-earth Van Vleck paramagnets with weak coupling is investigated both theoretically and experimentally. It is shown that the impurity relaxation is appreciably dependent on the fluctuation spectra of the host rare-earth ions. The line shapes of the fluctuation spectra are calculated using the method of moments for cases of interest. The role of the host exchange interaction and that of the rare-earth crystalline-field splitting in the relaxation process are demonstrated. The theory is applied to interpret the ESR linewidth behavior of Gd in the metallic Van Vleck paramagnets PrIn_3 (reported for the first time) as well as the linewidth behavior of Gd in the Van Vleck pnictides $\text{Pr}X$ ($X = \text{P, As, Sb, Bi}$) (reported previously and in the present work). The host exchange interaction in the pnictides was extracted by fitting the theory to the experimental ESR thermal broadening. These exchange parameters are compared with those estimated by means of other techniques. The rapid relaxation phenomenon in $\text{PrIn}_3\text{:Gd}$ is partially attributed to a relatively low-lying Γ_5 crystalline-field-splitting level in this system. The conduction-electron contribution to the relaxation rate is shown to be significant in $\text{PrIn}_3\text{:Gd}$ and $\text{LaIn}_3\text{:Gd}$. The exchange interaction between the Gd and conduction electrons was extracted in both systems.

I. INTRODUCTION

The magnetic properties of rare-earth inter-metallic compounds in which the rare-earth ions exhibit a singlet ground state have recently attracted considerable attention,^{1,2} especially those of the praseodymium Van Vleck compounds having cubic structure.³ The cubic crystalline field in these compounds splits the $J = 4$ multiplet of Pr^{+3} into a singlet ground state Γ_1 with two triplets Γ_4 and Γ_5 , and a doublet Γ_3 as excited states. As the singlet, Γ_1 , does not have a magnetic moment, many of these systems are nonmagnetic even at very low temperatures. This unique property enables one to observe the ESR signals of other rare-earth impurities such as Gd,⁴⁻⁸ Er,⁸ Yb, and Dy,⁹ in Van Vleck compounds. Such measurements might yield valuable information concerning the fluctuation spectra in singlet-ground-state systems.

We shall first give a brief review of the magnetic properties of singlet-ground-state systems. For more detailed discussion the reader is referred to several review papers such as that of Cooper and Vogt¹⁰ or that of Birgeneau.¹¹ It has been demonstrated by many authors^{2,3,10,11} that the presence of exchange interaction between the host praseodymium ions might lead to the formation of excitation bands in the Van Vleck compounds. These excitations have been treated by two types of models¹⁰ usually referred to as the "singlet-singlet"² and the "singlet-triplet"¹⁰ excitation models. In the framework of these models, it is

entirely possible to have a magnetic phase transition in a singlet-ground-state system provided that the nearest-neighbor exchange parameter \mathcal{J} exceeds the crystalline field splitting Δ . This phase transition is accompanied by softening of some of the excitation modes. In the "singlet-singlet" model, a phase transition will occur if the following condition is satisfied: $\eta \geq 1$, with a parameter η defined as

$$\eta = 4z_0 \mathcal{J}c^2/\Delta, \quad (1)$$

where z_0 is the number of Pr first nearest-neighbors, and c is a matrix element of the z component of the total angular momentum J connecting the singlet ground state with the first excited state. In view of the "excitation picture" it is useful to distinguish between two limiting cases: (i) "Strongly coupled" Van Vleck paramagnets characterized by a parameter η , defined by (1), very close to 1. In this case, a softening of some of the excitation modes occurs at low temperatures, even in the absence of a magnetic phase transition.² (ii) "Weakly coupled" Van Vleck compounds for which the condition $\eta \ll 1$ is satisfied. In this case the "excitations" form a very narrow excitation band located near Δ .

The present paper discusses some theoretical aspects of the fluctuation spectra in "weakly coupled" cubic Van Vleck paramagnets with emphasis on the ESR of impurities. In addition, we present new experimental data on the "weakly coupled" Van Vleck paramagnets $\text{Pr}_x\text{La}_{1-x}\text{In}_3$, Gd ,¹² and a

reanalysis of the Gd ESR linewidth in the Van Vleck pnictides, measured by others^{4,6} as well as in the present work. We shall not treat the case of "strongly coupled" Van Vleck paramagnets, as, to the best of our knowledge, no satisfactory ESR study of impurity exists for this limit at present.

The problem of fluctuations in the relaxation of impurities in cubic singlet-ground-state systems has been considered by several authors.^{5,4} Davidov, Rettori, and Zevin⁵ have suggested a phenomenological model based on the Bloch-Redfield kinetic equations.¹³ They have considered the spin-flip fluctuations of the host paramagnetic ions but have neglected any contribution to the impurity relaxation originating with modulation of the Zeeman levels produced by the z component of the fluctuations. Sugawara, Huang, and Cooper⁴ have adopted the theory of Moriya and Obata¹⁴ to interpret the ESR relaxation of Gd ions in several Van Vleck pnictides. Sugawara *et al.*⁴ argued that the impurity relaxation rate is proportional to the difference of the isothermal and the isolated susceptibilities of the host materials. According to Moriya and Obata,¹⁴ this is true provided that the impurity resonance frequency is far away from the resonance frequencies of the host paramagnetic ions. This last condition failed to exist in the case of Gd-doped Van Vleck pnictides of praseodymium, as the resonance frequency associated with the excited Γ_5 level of the host Pr is very close to that of the Gd.^{6,14} In the frame of the Bloch-Redfield kinetic equations, the approach of Sugawara *et al.*⁴ is equivalent to ignoring the spin-flip fluctuations and considering the modulation effect only. Both the approach of Davidov *et al.*⁶ and that of Sugawara *et al.*⁴ are phenomenological and do not give explicit expressions for the relaxation.

We use here the Bloch-Wangsness-Redfield equations to calculate the impurity relaxation in Van Vleck paramagnets.^{15,16} We show that the impurity relaxation is explicitly dependent on the line shape of the fluctuation spectra of the host Pr ions. Several cases for impurity relaxation are considered. The first case (case *a*) assumes that the width of the fluctuation spectra $\Delta\omega$ is much larger than the impurity resonance frequency ω_0 but smaller than the crystalline-field splitting ($\omega_0 \ll \Delta\omega < \Delta$). The line shape of the low-frequency part of the fluctuation spectra was calculated, for case *a*, using the method of moments. We demonstrate that both the second moment M_2 and the fourth moment M_4 of the low-frequency part of the fluctuation spectra are temperature dependent. The temperature dependence of M_2 should manifest itself in the relaxation rate of the magnetic im-

purity. As a result, the ESR thermal broadening of the magnetic impurity *does not* reflect, in a simple manner, the population of the excited Γ_4 and Γ_5 levels as previously assumed.^{4,6} The second limit (case *b*) assumes that the width of the fluctuation spectra $\Delta\omega$ is of the order of or even smaller than ω_0 , but still larger than the impurity relaxation rate $1/T_2$ ($\omega_0 \gtrsim \Delta\omega > 1/T_2$). In this case, a structure in the fluctuation spectra is expected. The second moments $M_2(\Gamma_4)$ and $M_2(\Gamma_5)$ associated with transverse fluctuations within the Γ_4 and Γ_5 multiplets, respectively, are calculated for case *b*. It is shown that at very low temperatures, $M_2(\Gamma_5)$ vanishes while $M_2(\Gamma_4)$ and M_2 exhibit finite values.

The limit $\Delta\omega \leq \omega_0$ in case *b* is usually not satisfied for the materials considered. This is because the host exchange interaction J is large enough to violate the requirement $\omega_0 > \Delta\omega$. There is, however, an intermediate case (case *c*) where J is large enough but nevertheless the fluctuation spectrum might exhibit a structure. The structure in the fluctuation spectrum in this case is a consequence of the different low-temperature properties of $M_2(\Gamma_5)$ with respect to those of M_2 and $M_2(\Gamma_4)$. Case *c* is favorable for materials which exhibit a low-lying Γ_5 level and for low temperatures.

Next, we present our experimental results on the system $\text{Pr}_x\text{La}_{1-x}\text{In}_3:\text{Gd}$ ($0 \leq x \leq 1$). The ESR spectra of $\text{PrIn}_3:\text{Gd}$ exhibit a large positive and temperature independent g shift in the temperature range between 1.4 and 20 K. The linewidth increases linearly with an increase in temperature at low temperatures, but reveals a large deviation from linearity above $T = 12$ K. While the initial linear increase of the linewidth versus temperature is attributed to conduction-electron effects, the deviation above 12 K is associated with the host magnetic ion's fluctuations according to our theory. We offer some evidence that the Γ_5 level is responsible for the relaxation phenomena (above $T \cong 12$ K). The very narrow range over which measurements were performed does not allow conclusive decision with respect to the dominant mechanism (case *a* or case *c*) in $\text{PrIn}_3:\text{Gd}$. The relaxation in the pnictides is interpreted using case *a*.

Section II of this paper describes our theory for impurity relaxation in "weakly coupled" Van Vleck paramagnets. Section III contains our experimental results on the $\text{Pr}_x\text{La}_{1-x}\text{In}_3:\text{Gd}$ ($0 \leq x \leq 1$) system as well as an analysis of this system and that of the pnictide series. We were able to extract the exchange interaction of the Gd ions with the host Pr ions and with the conduction electrons in PrIn_3 . The conduction-electron contribution was com-

pared to that in the isostructural compound $\text{LaIn}_3:\text{Gd}$. An attempt was also made to extract the host exchange interaction from both the ESR g shift of Gd in $\text{Pr}_x\text{La}_{1-x}\text{In}_3$ and the susceptibility of $\text{Pr}_x\text{La}_{1-x}\text{In}_3$. Finally, we demonstrate in Sec. III that fitting the theory to experiment enables one to extract the host exchange interaction \mathcal{J} from the impurity ESR linewidth. This is true if the crystalline-field levels are known from independent measurements. It provides us with a powerful technique for the study of \mathcal{J} in the Van Vleck pnictides. The values of \mathcal{J} extracted by us for the pnictide series are compared with those derived by others¹⁷ from combined susceptibility and neutron scattering data.¹⁸ The discussion in Sec. IV gives a comparison between the relaxation phenomenon in the pnictides and that in $\text{PrIn}_3:\text{Gd}$.

II. THEORY

A. Model

We shall mainly concentrate, at present, on praseodymium intermetallic compounds having cubic structure. The spin Hamiltonian describing the Pr ions can be written

$$\mathcal{H} = \mathcal{H}_{cf} + \mathcal{H}_{ex} + \mathcal{H}_Z, \quad (2)$$

where \mathcal{H}_{cf} is the crystalline-field Hamiltonian, \mathcal{H}_{ex} is the isotropic exchange interaction between the host Pr ions, and \mathcal{H}_Z is the Zeeman Hamiltonian. The Hamiltonians \mathcal{H}_{cf} , \mathcal{H}_{ex} , and \mathcal{H}_Z are given by¹⁹

$$\mathcal{H}_{cf} = \sum_k [B_4 O_4(\vec{J}^{(k)}) + B_6 O_6(\vec{J}^{(k)})], \quad (3)$$

$$\mathcal{H}_{ex} = -\frac{1}{2} \sum_{i \neq k} \mathcal{J}_{ik} \vec{S}_i \cdot \vec{S}_k = -\frac{1}{2} \sum_{i \neq k} \vec{\mathcal{J}}_{ik} \vec{J}^{(i)} \cdot \vec{J}^{(k)}, \quad (4)$$

with

$$\vec{\mathcal{J}}_{ik} = (g_J - 1)^2 \mathcal{J}_{ik}, \quad \mathcal{H}_Z = \sum_k g_J \mu_B \vec{H} \cdot \vec{J}^{(k)}, \quad (5)$$

where $O_4(\vec{J}^{(k)})$ and $O_6(\vec{J}^{(k)})$ are equivalent operators of the fourth degree and the sixth degree, respectively,²⁰ B_4 and B_6 are crystalline-field parameters of the fourth degree and sixth degree, respectively, \mathcal{J}_{ik} is the exchange interaction between the i th and k th Pr host ions, μ_B is the Bohr magneton, g_J is the Landé g factor, $\vec{J}^{(k)}$ is the total angular momentum of the k th Pr host ion, and \vec{H} is the external magnetic field. We have neglected in (2) any spin-spin interactions originating with dipole-dipole or quadrupole-quadrupole interactions, as these interactions are believed to be much smaller with respect to the exchange interaction (4). We have also neglected any anisotropy in the exchange Hamiltonian as well as conduction-electron contribution. The wave functions

appropriate to the various crystalline-field levels have been calculated by Lea, Leask and Wolf²¹ using (3). These wave functions are tabulated in Table I for the $J = 4$, $4f^2$ manifold of Pr^{+3} .

The impurity interacts with the neighboring host Pr ions via an exchange Hamiltonian of the form (4). For simplicity, however, we shall take into consideration only the first-neighbor Pr ions to each impurity ion. In this case, the exchange Hamiltonian \mathcal{H}'_{ex} between the impurity and the host Pr ions can be written

$$\mathcal{H}'_{ex} = - (g_J - 1) \mathcal{J}' \sum_{k=1}^{z_0} \vec{S} \cdot \vec{J}^{(k)}, \quad (6)$$

where \vec{S} is the spin of the impurity, \mathcal{J}' is the exchange interaction between the impurity and the host Pr ions, and z_0 is the number of the Pr first-neighbor ions to each impurity. The relaxation rate of this impurity can be calculated under the assumption that the impurity does not create a perturbation of the host Pr Hamiltonian. We have assumed, also, that the host spin system is a dissipative one.¹³ This assumption is equivalent to the requirement that the impurity ESR linewidth $1/T_2$ is much smaller with respect to the width of the host fluctuation spectra $\Delta\omega$. Furthermore, we restrict ourselves to a spin $S = \frac{1}{2}$ for the impurity. Under these assumptions, the Born approximation in the kinetic equations together with (2) yield the following expression for the impurity linewidth^{6,15,16} (see Appendix A):

$$1/T_2 = (\pi/2\hbar^2) (\mathcal{J}')^2 z_0 (g_J - 1)^2 \times [2K_{zz}(\omega_0) + K_{xx}(\omega_0) + K_{yy}(\omega_0)], \quad (7)$$

where ω_0 is the impurity resonance frequency. The spectral functions $K_{pp}(\omega)$ ($p = x, y, z$) are defined as (see also Appendix A)

$$K_{pp}(\omega) = \frac{1}{2\pi} \int_{-\infty}^{+\infty} \langle \delta J_p^{(k)}(t) \delta J_p^{(k)} \rangle e^{i\omega t} dt. \quad (8)$$

TABLE I. Wave functions appropriate to the various multiplets of Pr^{+3} in cubic crystalline field. These wave functions were calculated by Lea, Leask, and Wolf.

Level	Functions
Γ_1	$ \Gamma_1\rangle = 0.4564 4\rangle + 0.7638 0\rangle + 0.4564 -4\rangle$
Γ_4	$ \Gamma_4, a\rangle = 0.7071 4\rangle - 0.7071 -4\rangle$ $ \Gamma_4, b\rangle = 0.3536 3\rangle + 0.9354 -1\rangle$ $ \Gamma_4, c\rangle = 0.3536 -3\rangle + 0.9354 1\rangle$
Γ_3	$ \Gamma_3, a\rangle = 0.7071 2\rangle + 0.7071 -2\rangle$ $ \Gamma_3, b\rangle = 0.5401 4\rangle - 0.6455 0\rangle + 0.5401 -4\rangle$
Γ_5	$ \Gamma_5, a\rangle = 0.7071 2\rangle - 0.7071 -2\rangle$ $ \Gamma_5, b\rangle = 0.9354 3\rangle - 0.3536 -1\rangle$ $ \Gamma_5, c\rangle = 0.9354 -3\rangle - 0.3536 1\rangle$

We have chosen the coordinate axis to be along the cubic axis. This yields $K_{pq}(\omega) = 0$ for $p \neq q$ in (7) from symmetry considerations. The auto-correlation function $\langle \delta J_p^{(k)}(t) \delta J_p^{(k)} \rangle$ is given by

$$\langle \delta J_p^{(k)}(t) \delta J_p^{(k)} \rangle = \text{Tr} \left[\rho(\mathcal{H}) e^{i\mathcal{H}t/\hbar} \delta J_p^{(k)} e^{-i\mathcal{H}t/\hbar} \delta J_p^{(k)} \right]. \quad (9)$$

Here $\rho(\mathcal{H})$ is the Gibbs distribution function and \mathcal{H} is defined by (2). δJ_p is the fluctuation in J_p and can be expressed as

$$\delta J_p = J_p - \langle J_p \rangle \quad (p = x, y, z), \quad (10)$$

where $\langle J_p \rangle$ is the thermal average of J_p . In the absence of an external magnetic field $\langle J_p \rangle$ ($p = x, y, z$) is equal to zero, and the three spectral functions in (7) are equal for cubic symmetry. The spectral functions $K_{xx}(\omega)$ and $K_{yy}(\omega)$ in (7) originate from the spin-flip process of the ex-

change interaction between the impurity spin and the host ions (transverse fluctuations). The spectral function $K_{zz}(\omega)$ is the modulation term; this term originates with the z component of the fluctuating magnetic field produced by the fluctuating host magnetic ions.

It is easy and instructive to calculate the spectral functions in the limit of vanishing host exchange interaction and then to introduce this exchange interaction in a phenomenological manner. Such an approach has been adopted previously by Davidov, Rettori, and Zevin.⁶ We note that in the limit of vanishing host exchange, the requirement of a dissipative system no longer holds. However, such a method might give the reader an insight into the nature of the fluctuation spectrum in several limiting cases. In the limit $\mathcal{H}_{\text{ex}} = 0$, and for an external magnetic field parallel to the z direction, we have calculated the spectral functions using (2), (3), (7), and (8) to be

$$K_{zz}(\omega) = \sum_{\alpha, f_\alpha} p_\alpha |\langle \Gamma_\alpha f_\alpha | J_z | \Gamma_\alpha f_\alpha \rangle|^2 \delta(\omega) + \sum_{\substack{\alpha \neq \beta \\ f_\alpha, f_\beta}} p_\alpha |\langle \Gamma_\alpha f_\alpha | J_z | \Gamma_\beta f_\beta \rangle|^2 \delta(\omega - \omega_{\alpha\beta}) \\ - \sum_{\substack{\alpha, \beta \\ f_\alpha, f_\beta}} p_\alpha p_\beta \langle \Gamma_\alpha f_\alpha | J_z | \Gamma_\alpha f_\alpha \rangle \langle \Gamma_\beta f_\beta | J_z | \Gamma_\beta f_\beta \rangle \delta(\omega), \quad (11)$$

$$K_{xx}(\omega) = \sum_{\substack{\alpha, \beta \\ f_\alpha, f_\beta}} p_\alpha |\langle \Gamma_\alpha f_\alpha | J_x | \Gamma_\beta f_\beta \rangle|^2 \delta(\omega - \omega_{\alpha\beta}), \quad (12)$$

where the indices α and β represent various crystalline-field levels, and f_α and f_β characterize various wave functions within the multiplet Γ_α and Γ_β , respectively. The wave functions $\langle \Gamma_\alpha f_\alpha |$ are given in Table I for $J = 4$, $4f^2$ manifold. The population factors p_α and the frequency $\omega_{\alpha\beta}$ are defined as

$$p_\alpha = e^{-E_\alpha/T} / Z, \quad (13)$$

with

$$Z = \sum_{\alpha, f_\alpha} e^{-E_\alpha/T}$$

and

$$\omega_{\alpha\beta} = [E(\Gamma_\alpha, f_\alpha) - E(\Gamma_\beta, f_\beta)] / \hbar, \quad (14)$$

where E_α in (13) are the energy levels appropriate to the various crystalline-field levels in the absence of external magnetic field; the energy $E(\Gamma_\alpha, f_\alpha)$ corresponds to the Zeeman level f_α within the multiplet Γ_α . In the presence of a magnetic field, $\omega_{\alpha\beta}$ depends also on the indices f_α and f_β but for simplicity these indices were dropped.

The last term in (11) is very small with respect to the first one and is zero for $\vec{H} = 0$. It is clearly seen from (11) that in the limit of vanishing host exchange the spectrum of $K_{zz}(\omega)$ consists of "peaks" at $\omega = 0$ and at $\omega_{\alpha\beta}$ ($\alpha \neq \beta$). As $\omega_{\alpha\beta}$ ($\alpha \neq \beta$) corresponds to transitions between different crystalline-field levels, these "peaks" occur at very high frequencies. The spectrum of $K_{xx}(\omega)$ [or $K_{yy}(\omega)$] consists of peaks at ω_{44} and ω_{55} as well as at high frequencies $\omega_{\alpha\beta}$ ($\alpha \neq \beta$). The frequencies ω_{44} and ω_{55} refer to transitions between Zeeman levels of the Γ_4 and the Γ_5 multiplets, respectively. It has been demonstrated⁶ that these transitions are the only transitions between Zeeman levels of the same multiplet which have nonvanishing matrix elements of J_x (or J_y). The frequencies ω_{44} and ω_{55} are defined as

$$\omega_{\alpha\alpha} = (g_\alpha + \Delta g) \mu_B H / \hbar \quad (\alpha = 4, 5), \quad (15)$$

where g_α ($\alpha = 4, 5$) is given by $g_J \langle \Gamma_\alpha b | J_z | \Gamma_\alpha b \rangle$ and Δg is the exchange induced g shift due to the exchange interaction J with the surrounding Pr ions ($\Delta g = 0$ in the limit $\mathcal{H}_{\text{ex}} = 0$). The values of g_4 and g_5 appropriate to the transition be-

tween Zeeman levels of the Γ_4 and the Γ_5 multiplets, respectively, have been calculated to be $g_4 = 0.5$ and $g_5 = 2$.⁶ The latter g value is very close to the Gd resonance frequency.

Figure 1(d) exhibits the low frequency part of $K_{xx}(\omega)$ and $K_{zz}(\omega)$ for the hypothetical case of vanishing host exchange interaction. Figure 1 is only a schematic description of the low-frequency part of the fluctuations and the scales in Fig. 1 are arbitrary.

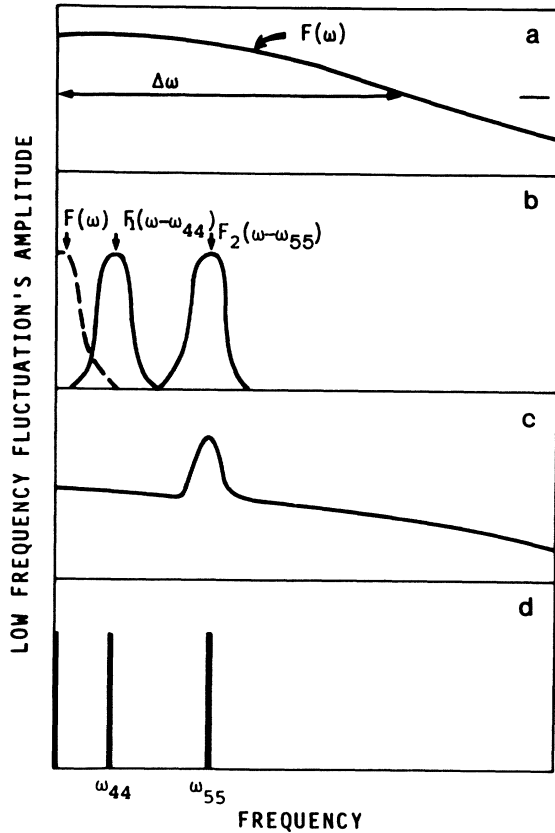


FIG. 1. Schematic description of the low-frequency part of the fluctuation spectra for several limiting cases. (a) The fluctuation spectra in the limit $\omega_0 \ll \Delta\omega < \Delta$ (case *a* in the text). (b) The fluctuation spectra in the limit $\Delta\omega < \omega_0$ (case *b*). The low-frequency part of the transverse fluctuations [$K_{xx}(\omega)$ and $K_{yy}(\omega)$] is given by the spectral functions $F_1(\omega - \omega_{44})$ and $F_2(\omega - \omega_{55})$ centered around $\omega = \omega_{44}$ and $\omega = \omega_{55}$, respectively. The low-frequency part of $K_{zz}(\omega)$ is given by the spectral function $F(\omega)$ centered around $\omega = 0$. This spectral function is described by a dashed line in Fig. (b). (c) The fluctuation spectra for the intermediate case (case *c* in the text). In this case the spectra exhibit a "peak" in the vicinity of $\omega = \omega_{55}$. (d) The spectra of fluctuation for the hypothetical case of vanishing host exchange interaction. It consists of δ function peaks at $\omega = 0$, $\omega = \omega_{44}$, and $\omega = \omega_{55}$. The former originates with the modulation term, the latter with the transverse fluctuations. The scales in Fig. 1 are arbitrary.

We shall introduce, now, the host exchange interaction, Eq. (4). In this case the δ functions in Eqs. (11) and (12) can be replaced by some distribution functions describing the low-frequency part of the fluctuation spectra.⁶ We shall demonstrate, later, that the width of these distribution functions is of the order of the host exchange interaction $z_0\mathcal{J}$. In the case of weakly coupled Van Vleck paramagnets [$z_0\mathcal{J} < \Delta$ according to (1)], this means no overlap between the high-frequency part and the low-frequency part of the fluctuation spectra.⁶ According to (7) the Gd relaxation rate is determined by the fluctuations at $\omega = 0$ and $\omega = \omega_0$ only. Thus only the low-frequency part of the fluctuation spectra is relevant to our problem. Several cases should be considered.

Case a. We can assume that $z_0\mathcal{J}$ is large enough such that the width of the distribution functions $\Delta\omega$ (describing the low-frequency part of the fluctuation spectra) is much larger than the impurity resonance frequency ω_0 . In this limit ($\Delta\omega \gg \omega_0$) it is impossible to distinguish between the transverse and the longitudinal components of the low-frequency part of the fluctuation spectra. This is due to the fact that ω_{44} and ω_{55} (as well as ω_0) are also smaller than $\Delta\omega$ and the effect of the external magnetic field on the fluctuation spectra can be neglected. Note that in the absence of external field $K_{zz}(\omega)$ and $K_{xx}(\omega)$ are the same for cubic symmetry [see also (11) and (12)]. Thus one can write

$$K_{zz}(0) = K_{yy}(0) = K_{xx}(0)$$

and also

$$K_{xx}(\omega_0) \cong K_{xx}(0), \quad K_{yy}(\omega_0) \cong K_{yy}(0).$$

It is instructive, therefore, to describe the low-frequency part of the fluctuation spectra by a single distribution function $F(\omega)$. Figure 1(a) exhibits the low-frequency part $F(\omega)$ for case *a*.

Case b. The width of the distribution functions $\Delta\omega$ is of the order of (or even smaller than) the resonance frequency ω_0 but is still larger than $1/T_2$. In this case one expects a structure in the transverse fluctuation spectra. This structure is associated with transition between the Zeeman levels of the Γ_4 and Γ_5 multiplets. In the limit of a very small host exchange ($\Delta\omega < \omega_0$), the low-frequency part of the transverse fluctuation spectra can be described by a function $F_1(\omega - \omega_{44})$ centered around $\omega = \omega_{44}$ and $F_2(\omega - \omega_{55})$ centered around $\omega = \omega_{55}$. The normalized low-frequency part of $K_{zz}(\omega)$ is represented by a function $F(\omega)$ centered around $\omega = 0$.

Case c. This is another interesting case which should be considered. Let us start with the limit

of vanishing host exchange ($\Delta\omega \ll \omega_0$) and let us increase \mathcal{J} gradually. It will be demonstrated below that the increase of \mathcal{J} is accompanied by an increase in the width of $F(\omega)$ and $F_1(\omega - \omega_{44})$. The width of $F_2(\omega - \omega_{55})$, however, remains relatively small at low temperatures. Thus, for the low-lying Γ_5 level, we expect the total fluctuation spectra to exhibit a structure (in a form of a "peak" at $\omega = \omega_{55}$) for low temperatures. This occurs even in the presence of large \mathcal{J} .

The low-frequency part of the fluctuation spectra for cases *b* and *c* are shown in Figs. 1(b) and 1(c), respectively. We shall now calculate the relaxation rate, $1/T_2$, for the various cases considered here.

B. Calculation of $1/T_2$ in the limit $\omega_0 \ll \Delta\omega < \Delta$ (case *a*)

In this limit $K_{xx}(\omega_0) = K_{yy}(\omega_0) \cong K_{zz}(0)$ and (7) is reduced to the following formula:

$$1/T_2 = (2\pi/\hbar^2) [\mathcal{J}'(g_J - 1)]^2 z_0 K_{zz}(0). \quad (16a)$$

Let us define a distribution function $F(\omega)$ with the property

$$F(\omega) = K_{zz}^{(LF)}(\omega) \left(\int_{-\infty}^{+\infty} K_{zz}^{(LF)}(\omega) d\omega \right)^{-1}, \quad (16b)$$

where $K_{zz}^{(LF)}(\omega)$ is the low-frequency part of $K_{zz}(\omega)$. With this definition one finds using (16b)

$$K_{zz}(0) = K_{zz}^{(LF)}(0) = F(0) \int_{-\infty}^{+\infty} K_{zz}^{(LF)}(\omega) d\omega. \quad (16c)$$

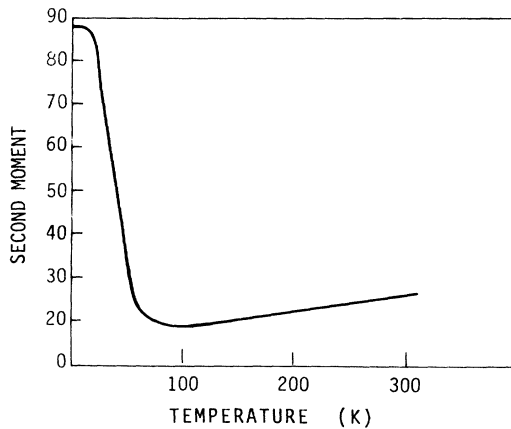


FIG. 2. Temperature dependence of the second moment

$$M_2 / \sum_{k \neq 1} (\bar{\mathcal{J}}_{1k})^2.$$

The second moment was calculated using (18) for the Van Vleck pnictide PrSb. The crystalline-field energy levels of PrSb were taken from Table III. The second moment for the other Van Vleck pnictides exhibits similar temperature dependence.

It is shown in Appendix B that [see Eq. (B8)]

$$\int_{-\infty}^{+\infty} K_{zz}^{(LF)}(\omega) d\omega = \sum_{\alpha=4,5} p_\alpha |\langle \Gamma_\alpha f_\alpha | J_z | \Gamma_\alpha f_\alpha \rangle|^2. \quad (16d)$$

This yields for (16a) the following expression:

$$\frac{1}{T_2} = \frac{2\pi}{\hbar^2} (J')^2 z_0 (g_J - 1)^2 F(0) \times \sum_{\alpha=4,5} p_\alpha |\langle \Gamma_\alpha f_\alpha | J_z | \Gamma_\alpha f_\alpha \rangle|^2. \quad (16e)$$

Expression (16e) is very similar to that used by Sugawara *et al.*⁴ to interpret their results. Sugawara *et al.* have assumed, however, that the factor $F(0)$ is temperature independent and have determined its magnitude by fitting this expression to the experimental results. In the present work we shall demonstrate that $F(0)$ can be calculated by the method of moments. On the assumption of a Gaussian line shape for $F(\omega)$, the second moment M_2 of $F(\omega)$ is related to $F(0)$ according to

$$F(0) = 1/(2\pi M_2)^{1/2}. \quad (17)$$

This calculation is carried out in Appendix B. The results clearly show that $F(0)$ is temperature dependent and the assumptions of Sugawara *et al.* are valid only for certain temperature ranges.

In calculating the second moment, M_2 , we started with the second moment of $K_{zz}(\omega)$ and have used the procedure of truncation. This was necessary because the second moment of $K_{zz}(\omega)$ contains contributions originating with the high-frequency part of the spectrum. This truncation is possible in the present case, as no overlap exists between the low-frequency part and the high-frequency part of the fluctuation spectra in the limit $\Delta\omega < \Delta$; ($\Delta = E_4$). The analytical method for this truncation was developed by McMillan and Opechowski²² using the projection operator technique.²³ Zevin and Shanina²⁴ solved the problem for the case of degenerate spectrum of the individual ion. We have adopted the method of Zevin and Shanina to calculate M_2 . Detailed calculations are given in Appendix B; here we quote our results. We found for M_2 the following expression:

TABLE II. Crystalline-field energy levels for Pr^{3+} in PrP, PrAs, PrSb, and PrBi as measured by neutron scattering technique.

Sample	E_4 (K)	E_3 (K)	E_5 (K)
PrP	125	215	394
PrAs	115	190	355
PrSb	73	125	239
PrBi	67	95	200

$$M_2 = \left(\sum_{i \neq 1} (\bar{\mathcal{J}}_{1i})^2 [Z (c_{44}^2 + c_{55}^2 e^{-(E_5 - E_4)/T})]^{-1} \right) \{ 2c_{44}^2 c_{14}^4 + 4c_{44}^6 e^{-E_4/T} + 4[(c_{44}^2 + c_{55}^2)(c_{44}^2 c_{55}^2 + c_{45}^4) + (c_{44} - c_{55})^2 c_{45}^4] e^{-E_5/T} + 2c_{44}^2 c_{43}^4 e^{-E_3/T} + 4c_{55}^6 e^{-(2E_5 - E_4)/T} + 2c_{55}^2 c_{53}^4 e^{-(E_5 + E_3 - E_4)/T} \}, \quad (18)$$

where $c_{\alpha\beta}$ represent various matrix elements for transitions between the crystalline-field levels of Pr^{+3} , $J=4$ multiplet. As the irreducible representation Γ_α appears only once in the $J=4$ representation, the values of $c_{\alpha\beta}$ are the same for all Pr compounds having cubic structure. The values of $c_{\alpha\beta}$ are given by

$$\begin{aligned} c_{14} &= \langle \Gamma_1 | J_z | \Gamma_4, a \rangle = 2(\frac{5}{3})^{1/2}, \\ c_{44} &= \langle \Gamma_4, b | J_z | \Gamma_4, b \rangle = -\frac{1}{2}, \\ c_{34} &= \langle \Gamma_3, b | J_z | \Gamma_4, a \rangle = 2(\frac{2}{3})^{1/2}, \\ c_{35} &= \langle \Gamma_3, b | J_z | \Gamma_5, a \rangle = 2, \\ c_{45} &= -\langle \Gamma_4, c | J_z | \Gamma_5, c \rangle = \frac{1}{2}(7)^{1/2}, \\ c_{55} &= \langle \Gamma_5, b | J_z | \Gamma_5, b \rangle = \frac{5}{2}. \end{aligned} \quad (19)$$

Figure 2 exhibits the second moment $M_2 / \sum (\bar{\mathcal{J}}_{1i})^2$ as a function of temperature for the special case of the Van Vleck compound PrSb. The value of $M_2 / \sum (\bar{\mathcal{J}}_{1i})^2$ was calculated using (18) together with the crystalline-field levels given in Table II. It is clearly seen that M_2 is temperature dependent [see also (18)]. This means that the relaxation rate $1/T_2$ does not reflect only the relative populations of the excited Γ_4 and Γ_5 levels as assumed by Sugawara *et al.*⁴ The various terms in (18) describe "two-ion" processes in which one ion undergoes a transition $|\Gamma_\alpha f_\alpha\rangle \rightarrow |\Gamma_\beta f_\beta\rangle$ ($\alpha \neq \beta$) and another ion simultaneously undergoes a transition $|\Gamma_\beta f_\beta\rangle \rightarrow |\Gamma_\alpha f_\alpha\rangle$. The probability that these transitions will take place is equal to $c_{\alpha\beta}^4$ multiplied by the relative weight of this transition. The mutual spin-flip process occurs via the exchange.

Myers and Narath²⁵ have recently calculated the relaxation rate of the host nuclei as measured by NMR in weakly coupled Van Vleck paramagnets. They used a model with an effective spin $\frac{1}{2}$, taking into consideration only a two-level scheme: the singlet ground state and an excited state. Their results are identical to ours in the limit $T=0$. Thus, the model of Myers and Narath²⁵ is valid only for very low temperatures. As is clearly seen from Fig. 2, M_2 decreases appreciably upon increasing the temperatures. This might change the fitting of Myers and Narath in the high-temperature range.

It should be pointed out that (17) holds provided that $F(\omega)$ has a Gaussian line shape. Some information concerning the exact line shape of $F(\omega)$ can be gained by performing calculations of the fourth moment M_4 . It is well known from the theory of

moments in ESR that the ratio $M_4/3(M_2)^2$ should be equal to 1 for a Gaussian distribution but much larger than 1 for a Lorentzian.

In Appendix C we present a general formula for the fourth moment M_4 of $F(\omega)$. This formula contains many terms originating with "two-ion processes," as well as from three- and four-ion processes. It should be pointed out that in the calculation of the second moment M_2 (see Appendix B) all the processes in which more than two ions are involved were cancelled out. In view of the complicated expression for M_4 we shall give here only its value in the limit $T \rightarrow 0$. We found for the rocksalt structure

$$M_4(T \approx 0) = (\bar{\mathcal{J}})^4 z_0 (6 z_0 + 30) c_{14}^8. \quad (20)$$

In the same limit we have calculated $M_4/3(M_2)^2$ to be

$$M_4(T=0)/3[M_2(T=0)]^2 = 0.7. \quad (21)$$

This indicates that at low temperatures ($T \ll \Delta$) the line shape of $F(\omega)$ is very close to a Gaussian line shape. In estimating (20) and (21), we have made the approximations

$$\sum_{i \neq 1} (\mathcal{J}_{1i})^2 = z_0 (\mathcal{J})^2 \quad \text{and} \quad \sum_{i \neq 1} (\mathcal{J}_{1i})^4 = z_0 (\mathcal{J})^4,$$

etc.

Knowledge of the line shape of $F(\omega)$ as a function of temperature requires a computer calculation of M_4 and $M_4/3(M_2)^2$. Our preliminary calculation (to be published elsewhere) indicates that the ratio $M_4/3(M_2)^2$ varies with temperature. In the present work we shall assume, however, that the line shape is Gaussian. This is consistent with the approach of Myers and Narath²⁵ who used a Gaussian line shape for the fluctuation spectra to interpret the relaxation of the ³¹P nucleus in PrP. Finally, pair correlation contributions to M_2 have been calculated (to be published elsewhere) and were found to be less than 30% of the autocorrelation contribution calculated in the present work.

C. Calculation of $1/T_2$ in the limit $\Delta\omega \lesssim \omega_0$ (case b)

In the limit $\Delta\omega < \omega_0$ the low-frequency parts of the fluctuation spectra consists of broad but separated peaks. The low-frequency parts of the spectral functions $K_{xx}(\omega_0)$ and $K_{zz}(\omega_0)$ can be expressed in this limit as

$$K_{xx}(\omega_0) = (2/Z) [e^{-E_4/T} |\langle \Gamma_4, a | J_x | \Gamma_4, c \rangle|^2 F_1(\omega_0 - \omega_{44}) + e^{-E_5/T} |\langle \Gamma_5, a | J_x | \Gamma_5, c \rangle|^2 F_2(\omega_0 - \omega_{55})], \quad (22)$$

$$K_{zz}(0) = [2F(0)/Z] (e^{-E_4/T} |\langle \Gamma_4 b | J_z | \Gamma_4 b \rangle|^2 + e^{-E_5/T} |\langle \Gamma_5 b | J_z | \Gamma_5 b \rangle|^2), \quad (23)$$

where $F_1(\omega_0 - \omega_{44})$ and $F_2(\omega_0 - \omega_{55})$ represent the amplitude of the normalized spectral functions, originating with transverse fluctuations, within the Γ_4 and Γ_5 multiplets at the impurity resonance frequency ω_0 . These functions are centered around ω_{44} and ω_{55} defined by (15). $F(0)$ represents the amplitude of the low-frequency part of $K_{zz}(\omega)$ at $\omega = 0$. Combining (7) with (22) and (23) yields for $1/T_2$ the following expression:

$$\begin{aligned} 1/T_2 = & (2\pi/\hbar^2) (\mathcal{J}')^2 z_0 (g_J - 1)^2 \\ & \times [0.125 F_1^*(e^{-E_4/T}/Z) + 3.125 F_2^*(e^{-E_5/T}/Z)], \end{aligned} \quad (24)$$

where F_1^* and F_2^* are given by

$$\begin{aligned} F_1^* &= F_1(\omega_0 - \omega_{44}) + 2F(0), \\ F_2^* &= F_2(\omega_0 - \omega_{55}) + 2F(0). \end{aligned} \quad (25)$$

Formula (24) was derived under the assumption that $\omega_0 > \Delta\omega > 1/T_2$. It represents a generalization of the phenomenological approach of Davidov, Rettori, and Zevin to include the modulation contribution to $1/T_2$. The values of $F_1(\omega_0 - \omega_{44})$ and $F_2(\omega_0 - \omega_{55})$ in (25) and (24) are related to the second moments $M_2(\Gamma_4)$ and $M_2(\Gamma_5)$ associated with these spectral functions. The calculations of the second moments of $F_1(\omega - \omega_{44})$ and $F_2(\omega - \omega_{55})$ are given in Appendix D. We have used the projection operator technique in complete analogy with the calculation in Appendix A. The results for $(M_2)^{1/2} < \omega_{\alpha\alpha}$ are given by

$$\begin{aligned} M_2(\Gamma_4) = & \left(\sum_{i \neq 1} (\bar{\mathcal{J}}_{1i})^2 Z^{-1} \right) [2c_{14}^4 + 4c_{44}^4 e^{-E_4/T} + \frac{13}{8} c_{43}^4 e^{-E_3/T} \\ & + 2(c_{44}^2 c_{55}^2 + 2c_{45}^4) e^{-E_5/T}], \end{aligned} \quad (26a)$$

$$\begin{aligned} M_2(\Gamma_5) = & \left(\sum_{i \neq 1} (\bar{\mathcal{J}}_{1i})^2 Z^{-1} \right) [2(c_{44}^2 c_{55}^2 + 2c_{54}^4) e^{-E_4/T} \\ & + \frac{13}{8} c_{35}^4 e^{-E_3/T} + 4c_{55}^4 e^{-E_5/T}]. \end{aligned} \quad (26b)$$

For $(M_2)^{1/2} > \omega_{\alpha\alpha}$, we find

$$\begin{aligned} M_2(\Gamma_4) = & \left(\sum_{i \neq 1} (\bar{\mathcal{J}}_{1i})^2 Z^{-1} \right) [2c_{14}^4 + 4c_{44}^4 e^{-E_4/T} + 2c_{43}^4 e^{-E_3/T} \\ & + 4(c_{44}^2 c_{55}^2 + 2c_{45}^4) e^{-E_5/T}], \end{aligned} \quad (27a)$$

$$\begin{aligned} M_2(\Gamma_5) = & \left(\sum_{i \neq 1} (\bar{\mathcal{J}}_{1i})^2 Z^{-1} \right) [4(c_{44}^2 c_{55}^2 + 2c_{45}^4) e^{-E_4/T} \\ & + 2c_{35}^4 e^{-E_3/T} + 4c_{55}^4 e^{-E_5/T}]. \end{aligned} \quad (27b)$$

In Figs. 3(a) and 3(b) the temperature dependences of $M_2(\Gamma_4)$ and $M_2(\Gamma_5)$ for the case $(M_2)^{1/2} > \omega_{\alpha\alpha}$ are shown. It is clearly seen that while M_2 and $M_2(\Gamma_4)$ have a finite value at very low temperatures, the value of $M_2(\Gamma_5)$ is zero at $T = 0$. This property has a significant consequence with respect to the character of the fluctuation spectra in Van Vleck paramagnets exhibiting a low-lying Γ_5 state. This is discussed in Sec. IID.

D. Intermediate case (case c)

For the materials being considered the condition $\Delta\omega < \omega_0$ is usually not satisfied. This is a con-

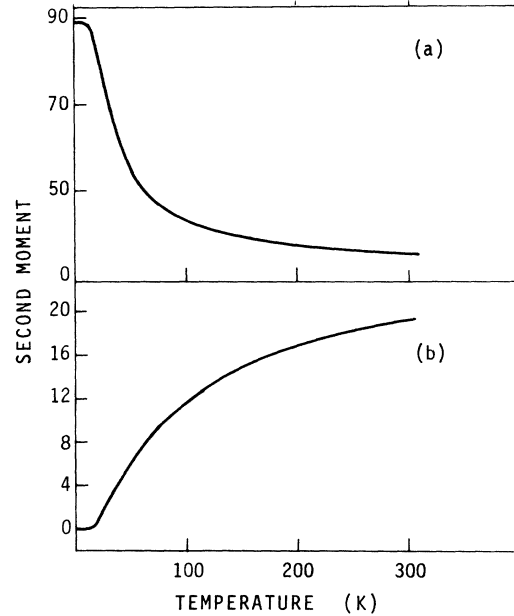


FIG. 3. The temperature dependence of the second moments (a)

$$M_2(\Gamma_4) / \sum_{k \neq 1} (\bar{\mathcal{J}}_{1k})^2$$

(b)

$$M_2(\Gamma_5) / \sum_{k \neq 1} (\bar{\mathcal{J}}_{1k})^2.$$

These second moments were calculated using Eqs. (27) and for PrSb.

sequence of the relatively large value of J (several degrees Kelvin) leading to a large value of $\Delta\omega$. There is, however, a situation where the fluctuation spectra exhibit a structure even in the presence of relatively large J . This can be understood in view of the different low-temperature properties of M_2 , $M_2(\Gamma_4)$, and $M_2(\Gamma_5)$: while M_2 and $M_2(\Gamma_4)$ exhibit a finite value at low temperatures, $M_2(\Gamma_5)$ is zero for $T=0$. The formation of structure in the fluctuation spectra at low temperatures can be explained as follows: In the limit of very small host exchange, the low-frequency part of the fluctuation spectra consists of the spectral functions $F(\omega)$, $F_1(\omega - \omega_{44})$, and $F_2(\omega - \omega_{55})$. Increasing J broadens $F(\omega)$ and $F_1(\omega - \omega_{44})$ significantly; the width of $F_2(\omega - \omega_{55})$ at low temperatures remains small. In the limit of large J , the low-temperature fluctuation spectra exhibit a structure at $\omega = \omega_{55}$ provided that the Γ_5 level is a low-lying state. This structure might manifest itself by a "peak" at $\omega = \omega_{55}$ situated above a background of fluctuations originating with $K_{zz}(\omega)$ and the transverse fluctuations within the other multiplet. For an impurity with a resonance frequency ω_0 close to ω_{55} , the relaxation is dominated by $F_2(\omega - \omega_{55})$. In this limit one can write for $1/T_2$ the following expression:

$$1/T_2 \cong (\pi/\hbar) (\mathcal{G}')^2 (g_J - 1)^2 z_0 \times (e^{-E_5/T}/Z) F_2(\omega_0 - \omega_{55}), \quad (28)$$

with

$$F_2(\omega_0 - \omega_{55}) = \{1/[2\pi M_2(\Gamma_5)]^{1/2}\} \times e^{-(\omega_0 - \omega_{55})^2/2M_2(\Gamma_5)}, \quad (29)$$

where $M_2(\Gamma_5)$ is defined by (26b) and (27b) and a Gaussian line shape for $F_2(\omega - \omega_{55})$ is assumed. The main assumption made in (28) is that the width $[2\pi M_2(\Gamma_5)]^{1/2}$ of $F_2(\omega - \omega_{55})$ is small enough to exhibit a significant peak at $\omega = \omega_{55}$ but wide enough such that the amplitude of $F_2(\omega - \omega_{55})$ at the impurity resonance frequency ω_0 is not negligible. Note that $\omega_0 \neq \omega_{55}$ at low temperatures (here ω_0 stands for the Gd resonance frequency) and the requirement of $F_2(\omega_0 - \omega_{55}) \neq 0$ is satisfied only above a certain temperature T_0 . Thus, below T_0 there will be no relaxation via the Γ_5 level since $F_2(\omega_0 - \omega_{55}) \cong 0$. As the temperature increases, there is a broadening of $F_2(\omega - \omega_{55})$ such that above T_0 , a new channel for the impurity relaxation is opened up. The relaxation rate (28) is valid only for $T > T_0$. This relaxation phenomenon is similar to the cross-relaxation mechanism described previously. At still higher temperatures, the width of $F_2(\omega - \omega_{55})$ is comparable to that of the low-frequency part of $K_{zz}(\omega)$ and the relaxation rate is determined by (16a) and (16e).

III. EXPERIMENT AND ANALYSIS

A. System $\text{Pr}_x\text{La}_{1-x}\text{In}_3$ (doped with Gd or undoped)

The system PrIn_3 is a metallic Van Vleck paramagnet having cubic structure. Specific-heat study²⁶ of this compound indicated that the ground state is a singlet Γ_1 with a triplet as a first excited state at an energy of 100 ± 30 K. A susceptibility study^{27,28} predicted the existence of a Γ_4 level at an energy of 110 ± 10 K. In view of this large splitting, it is believed that PrIn_3 is a weakly coupled Van Vleck paramagnet, although no accurate information concerning the host exchange exists at present.

This section presents an ESR study of Gd in $\text{PrIn}_3:\text{Gd}$ and $\text{LaIn}_3:\text{Gd}$. Measurements on the latter compound were necessary in order to determine the conduction-electron contribution to the g shift and linewidth. We have estimated, also, an upper limit to the host exchange from a susceptibility study of $\text{Pr}_x\text{La}_{1-x}\text{In}_3$ ($0 \leq x \leq 1$) as well as from the low-temperature ESR g shift of Gd in $\text{Pr}_x\text{La}_{1-x}\text{In}_3$. The $\text{Pr}_x\text{La}_{1-x}\text{In}_3$ samples, doped with Gd or undoped, were prepared in sealed tantalum tubings in a vacuum furnace or using an arc furnace. The ESR measurements were carried out mainly at X band. The susceptibility was measured using a vibrating-sample magnetometer. Our results and analysis are summarized below.

1. ESR of $\text{LaIn}_3:\text{Gd}$

The ESR measurements were carried out on powdered samples. The Gd concentrations were between 50 and 2000 ppm. A single line with a metallic line shape was observed. The field for resonance is appropriate to a g value of 2.039 ± 0.005 . The linewidth increased linearly with an increase in temperature and can be described by the formula $a + bT$; here a is the residual width and b is the thermal broadening. The values of a , b , and the g value for the various samples measured are exhibited in Table III. In addition, the temperature range over which the experiments were carried out is also indicated in the table. We attribute the g shift and the thermal broadening in $\text{LaIn}_3:\text{Gd}$ to the exchange interaction j between the Gd ions and the conduction electrons. In the absence of a bottleneck effect²⁹ in the relaxation mechanism, this g shift Δg_{CE} and the thermal broadening b originating with the conduction electrons can be expressed as

$$\Delta g_{\text{CE}} = j\eta, \quad (30)$$

$$bT = (\pi/g\mu_B) (j\eta)^2 K_B T, \quad (31)$$

where K_B is the Boltzmann factor and η is the con-

TABLE III. Thermal broadening b , the residual width a , and the g value as measured for various $\text{LaIn}_3\text{:Gd}$ samples. The temperature range over which the measurements were performed is indicated.

Gd concentration (ppm)	a (G)	b (G/K)	g value	Temperature range (K)
50	46	24 ± 5	2.038 ± 0.005	1.4–4.2
100	51	22 ± 4	2.040 ± 0.005	1.4–4.2
500	70	17 ± 6	2.041 ± 0.005	1.4–4.2
500	50	23 ± 4	2.043 ± 0.004	1.4–12
1000	60	20 ± 5	2.041 ± 0.005	1.4–10
2000	53	19	2.040 ± 0.005	1.4–4.2

duction-electron density of states per one spin direction. The value of η for LaIn_3 was measured by Welsh *et al.*³⁰ to be $\eta = 0.268$ states/eV spin atom. Using this value as well as (30) and (31), we have extracted the following exchange parameters

$$j_{\Delta g} = +0.14 \text{ eV}, \quad |j_b| = 0.11 \text{ eV}, \quad (32)$$

where $j_{\Delta g}$ and j_b are the exchange parameters derived from the g shift and the thermal broadening, respectively. We have neglected in our analysis the Coulomb interaction between the conduction electrons responsible for the exchange enhancement of the conduction-electron susceptibility. This is allowed according to the work of Welsh *et al.*³⁰ The exchange parameters derived by us in (32) are significantly larger than the exchange parameter of 0.032 eV estimated by Welsh *et al.*³⁰ from NMR relaxation of ^{139}La nucleus in LaIn_3 doped with Gd.

2. ESR of $\text{PrIn}_3\text{:Gd}$

ESR measurements were performed on powdered samples with Gd concentrations of 30 000, 4000 (two samples), and 1500 ppm. The spectra exhibit a single line with a metallic line shape at temperatures lower than 25 K. We found the Gd g value in PrIn_3 to be temperature independent in the range $1.4 \leq T \leq 4.2$ K and equal to $g = 2.40 \pm 0.01$ K. The linewidth versus temperature increases linearly with a rate of 16 ± 5 G/K at temperatures to approximately 10 K (Fig. 4). Above this temperature, the linewidth increases much more rapidly (Fig. 4). Above temperatures of approximately 25 K the ESR line becomes very broad and no longer exhibits a Lorentzian line shape. At 30 K (see Fig. 4) the "linewidth" (half width at half intensity) is of the order of 1500 G for the 3%-Gd sample. This width is of the order of the field for resonance at X-band frequency and makes the conventional analysis impossible. We were not able, therefore, to analyze the ESR spectrum

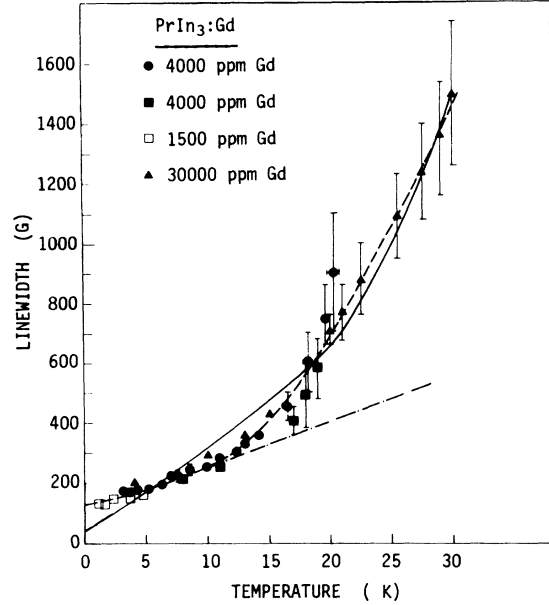


FIG. 4. ESR linewidth of Gd in PrIn_3 (for several Gd concentrations) as a function of temperature. The dashed line represents the linear initial thermal broadening. This initial thermal broadening is believed to originate with a Korringa-like mechanism. The solid line in Fig. 4 represents the best fit of case a , Eq. (16e), to the experimental results. The broken line represents the best fit of case c , Eq. (28) to the experimental linewidth. The second moment $M_2(\Gamma_3)$ was calculated using (27). In both cases the fit was done to the experimental linewidth at the high-temperature range. It is seen that Eq. (28) fits very well to the experiment over the entire temperature range studied. The second moments were calculated using (18) and (27), respectively, with the crystal-line-field levels as measured by Knorr, Murani, and Gross (see text).

for temperatures higher than 30 K (also at this temperature the experimental uncertainty is very large, see Fig. 4).

The g shift of Gd induced by the host Pr ions in metallic Van Vleck paramagnets is given by^{4,5}

$$\Delta g = [(g_J - 1)/g_J] \mathcal{J}' z_0 \chi_m / \mu_B^2 N_0, \quad (33)$$

where χ_m is the host Van Vleck susceptibility and N_0 is the Avogadro number. The g shift induced by the host Pr ions is obtained from the experimental g shift by subtracting the conduction-electron contribution. Assuming that the g shift originating with the conduction electrons is identical to that in $\text{LaIn}_3\text{:Gd}$ and using $\chi_m = 0.029$ emu/mol,²⁸ the value of $\mathcal{J}' z_0$ was extracted. We found that $\mathcal{J}' z_0 = -1.6$ meV. The negative sign of the exchange interaction \mathcal{J}' is in agreement with those observed previously for Gd in the heavy pnictides.^{4,5}

We turn, now, to the linewidth behavior in

PrIn₃:Gd. The initial linear increase of the linewidth versus temperature (Fig. 4) is attributed to a Korringa process due to the exchange interaction j between the Gd ions and the conduction electrons [see Eq. (31)]. This interpretation is supported by the very similar thermal broadening observed in the analogous compound LaIn₃:Gd. Furthermore, for a splitting of approximately 100 K between the singlet ground state and the excited triplet states, no significant contribution from the Pr fluctuation mechanism (7) to the Gd relaxation is expected below 5 K. Our experimental results, however, clearly show a large thermal broadening already below 4 K for PrIn₃:Gd (Fig. 4). Thus, we can use the Korringa relation to explain the initial increase of the linewidth in PrIn₃:Gd. Assuming the density of states of the conduction electrons in PrIn₃ to be identical to that of³⁰ LaIn₃ ($\eta = 0.268$ states/eV spin atom), we have estimated the exchange interaction between the Gd ions and the conduction electrons to be $j_b = 0.10$ eV. (The index b indicates that this exchange parameter was extracted from the experimental thermal broadening.)

The rapid thermal broadening above 12 K in Fig. 4 is attributed to fluctuations of the host Pr ions via (28). We shall leave this part until Sec. IV.

3. Susceptibility of Pr_xLa_{1-x}In₃

The susceptibility of PrIn₃ is shown in Fig. 5. Apart from a small paramagnetic contribution at

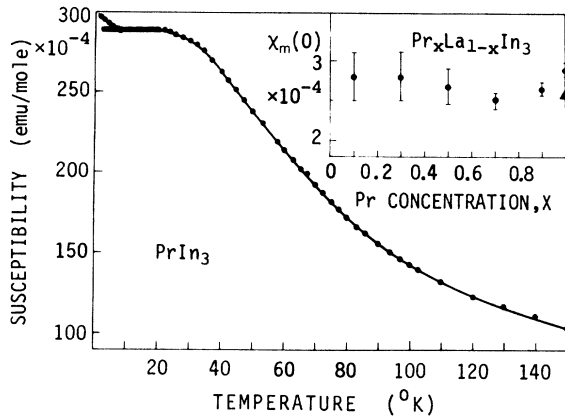


FIG. 5. Susceptibility of PrIn₃ as a function of temperature. The horizontal solid line at low temperatures reflects the temperature independence of the susceptibility in this temperature range as verified also from ESR g -shift study. The inset in Fig. 3, represents the low-temperature Van Vleck susceptibility $\chi_m(0)$ as a function of the Pr concentration x in Pr _{x} La_{1- x} In₃. $\chi_m(0)$ here is expressed in emu/mol%. The triangle in the inset represents the value of $\chi_m(0)$ as measured by others (see Ref. 27).

low temperatures, the susceptibility of PrIn₃ is almost constant in the temperature range between 1.4 and 25 K but decreases appreciably upon increasing the temperature above 25 K. The near temperature independence of the susceptibility in the range $1.4 \leq T \leq 25$ K is consistent with the temperature independence of the Gd g shift, as the latter reflects the host susceptibility according to (33). The small paramagnetic contribution at low temperatures is probably due to the presence of other rare-earth ions in the 99.9%-pure praseodymium.

The Van Vleck susceptibility at very low temperatures $\chi_m(0)$ can be expressed, assuming a molecular-field approximation, as

$$\chi_m(0) = \chi_c \left[1 - \mathcal{J} z_0 \left(\frac{g_J - 1}{g_J} \right)^2 \frac{\chi_c}{\mu_B^2 N_0} \right]^{-1}, \quad (34)$$

with χ_c defined as

$$\chi_c = x 2 g_J^2 \mu_B^2 N_0 c_{14}^2 / E_4, \quad (35)$$

where x in (35) is the Pr concentration in Pr _{x} La_{1- x} In₃ ($x = 1$ for PrIn₃). It is clearly seen from (34) and (35) that $\chi_m(0)$ depends on the host exchange interaction J as well as on the crystal-field level E_4 . The value of \mathcal{J} can be extracted, therefore, from a susceptibility study provided that the value of E_4 is known from an independent measurement (such as inelastic neutron scattering). Unfortunately, no such study is available at present and the specific-heat data do not yield a unique value for E_4 in PrIn₃. In the absence of this information, one can estimate J by measuring $\chi_m(0)$ as a function of x in Pr _{x} La_{1- x} In₃.

The susceptibility of several Pr _{x} La_{1- x} In₃ samples was measured as a function of temperature for various x values. The results exhibit similar features to those of PrIn₃ described in Fig. 5. The zero-temperature susceptibility, after subtracting the "dirt" paramagnetic impurities contribution, was extracted for the various samples measured. The inset in Fig. 5 gives the value of $\chi_m(0)$ (defined as the zero temperature susceptibility per 1 mol% of Pr) as a function of the Pr concentration in Pr _{x} La_{1- x} In₃. Our result in Fig. 5 indicates that the change in $\chi_m(0)$ does not exceed 10% and is not monotonic across the series. This is unlike previous measurements on²⁷ Pr _{x} La_{1- x} Pb₃ and³¹ Pr_{3- x} La _{x} Tl where a large and monotonic change in $\chi_m(0)$ was observed. Furthermore, the presence of "dirt" as well as the measurement uncertainties cause relatively large "error bars" mainly at the low-Pr-concentration range. This does not allow an accurate determination of \mathcal{J} , but might yield an upper limit to its value. We estimate $z_0 |\mathcal{J}| \leq 2.5$ meV. It should be stressed, also, that our analysis is based on the assumption that E_4 in (15)

does not change upon changing the Pr concentration. This assumption is not justified and might lead to our results in Fig. 5, especially if J is relatively small. Using the value $z_0|\mathcal{J}|\leq 2.5$ meV, we have estimated E_4 from (34) and (35) to be $E_4 = 105 \pm 10$ K. The uncertainty in E_4 is a result of the uncertainty in the sign and magnitude of J .

4. ESR of $\text{Pr}_x\text{La}_{1-x}\text{In}_3:\text{Gd}$

We have demonstrated in (30) that the Gd ESR g shift is proportional to the Pr host susceptibility χ_m . This susceptibility depends, according to (34) and (35), on the Pr concentration as well as on the value of \mathcal{J} . Thus, provided that \mathcal{J} is large enough, a nonlinearity of Δg vs the Pr concentration in $\text{Pr}_x\text{La}_{1-x}\text{In}_3:\text{Gd}$ is expected according to (33)–(35). This might yield information concerning the magnitude and sign of \mathcal{J} . Motivated by this point, we have performed an ESR study of Gd in $\text{Pr}_x\text{La}_{1-x}\text{In}_3$. The measurements were carried out in the helium temperature range. The spectra exhibit a single line with a linewidth and a line shape (A/B ratio in the notation of Fehr and Kip³²) varying appreciably with Pr concentration. While the spectra of $\text{PrIn}_3:\text{Gd}$ and $\text{LaIn}_3:\text{Gd}$ exhibit a “normal metallic line shape” with an A/B ratio of 2.5, the A/B ratio of the mixed phases, $\text{Pr}_x\text{La}_{1-x}\text{In}_3:\text{Gd}$ ($x \neq 0, 1$), is smaller and even close to 1 for several samples. The deviation from the “normal line shape” is usually accompanied by a broadening of the ESR lines. This behavior is probably associated with the formation of an internal field distribution in the mixed phase.

We have analyzed the ESR spectra using the method of Peter *et al.*³³ (or by fitting to a Dysonian line shape³²). The g shifts for the various samples are exhibited in Fig. 6. It is clearly seen that the g value increases almost linearly with the Pr concentration. This behavior confirms our susceptibility study above, that the susceptibility per Pr ion in $\text{Pr}_x\text{La}_{1-x}\text{In}_3$ is almost constant (within 15%). We were not able to extract a reasonable value of \mathcal{J} because of large “error bars” in our measurements (Fig. 6). However, from this study an upper limit to J can be estimated. We estimate $z_0|\mathcal{J}|\leq 2.5$ meV for PrIn_3 .

B. Pnictide series

The linewidths of $\text{Pr}X:\text{Gd}$ ($X = \text{P}, \text{As}, \text{Sb}, \text{Bi}$) have been measured as a function of temperature by Sugawara *et al.*⁴ Some measurements were also performed on $\text{PrSb}:\text{Gd}$ by Davidov *et al.*⁶ In the present paper, we have remeasured the ESR linewidth of Gd in PrSb and PrBi . This was necessary because of a slight disagreement between theory and experiment in the low-temperature

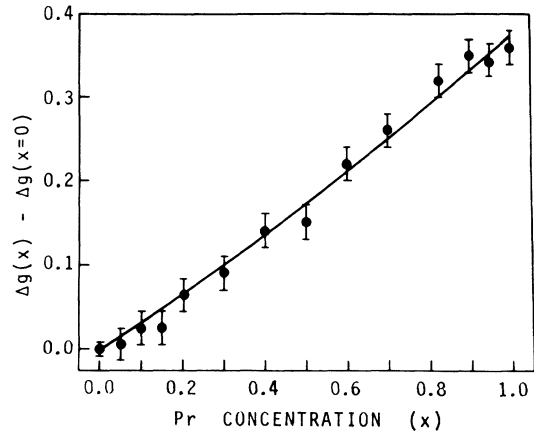


FIG. 6. g shift of Gd in $\text{Pr}_x\text{La}_{1-x}\text{In}_3$ as a function of the Pr concentration x at a constant temperature of $T=4.2$ K. The g shift is measured with respect to that found for Gd in LaIn_3 ($g=2.040$).

range (see discussion below). We found our data to be consistent with those of Sugawara *et al.*⁴ provided that residual widths of 260 and 400 G are assumed for $\text{PrSb}:\text{Gd}$ (with 1% Gd) and $\text{PrBi}:\text{Gd}$ (1.5% Gd), respectively. (In the original plot of Sugawara *et al.* the residual width was already subtracted.) Figures 7–10 exhibit the linewidth versus temperature (after subtracting the residual width) as measured by Sugawara *et al.*⁴ and by the present authors.

In analyzing the linewidth behavior, several

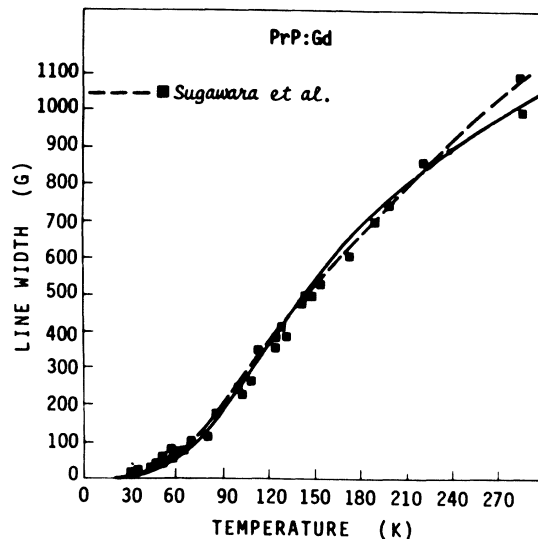


FIG. 7. Linewidth (after subtracting the residual width) of Gd in PrP as a function of temperatures. The squares represent the experimental data taken by Sugawara *et al.* The solid line represents the best fit of (16e) to the experimental data. The dashed line is the fit of Sugawara *et al.*

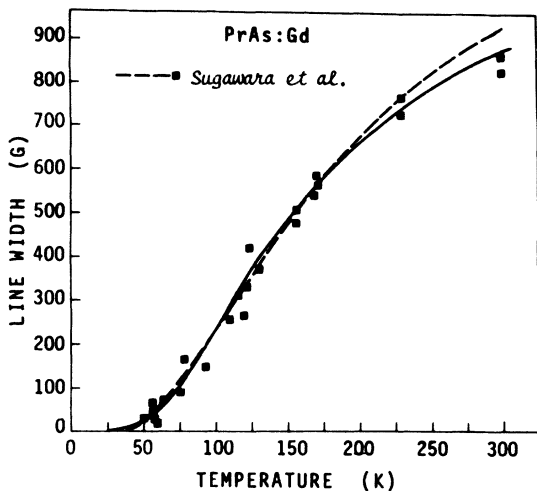


FIG. 8. Linewidth (after subtracting the residual width) of Gd in PrAs as a function of temperature. The solid line represents the best fit of (16e) to the experimental data (the squares in Fig. 8). For comparison, the fit of Sugawara *et al.* is given by the dashed line in this figure.

points should be taken into consideration. First, the host exchange in these compounds is of the order of several degrees Kelvin.¹⁷ Assuming a Gaussian distribution of fluctuations, this would lead to a width $\Delta\omega$ of the order of 10^5 G. This width is larger than the Gd field for resonance but smaller than the crystalline-field splitting. Second, no significant perturbation of the fluctuation spectra due to the Γ_5 level is expected. This is owing to the relatively large value of E_5 (Table III) leading to its small population factor at low temperatures. These arguments might indicate that the Pr fluctuation spectra in the pnictide series exhibit the property $\Delta > \Delta\omega \gg \omega_0$ (case *a*). Under this assumption, the Gd relaxation rate in Van Vleck pnictides is determined by Eq. (16e).

The solid lines in Figs. 7–10 are the best theoretical fit of (16e) to the high-temperature experimental linewidth. For comparison, the fits of Sugawara are also given by the dashed lines in these figures. It is clearly seen that a reasonable agreement between theory and experiment exists for the Van Vleck compounds PrP:Gd and PrAs:Gd over all temperature ranges (Figs. 7 and 8). There is, however, some deviation of theory from experiment for the heavy pnictides and especially for PrBi:Gd at low temperatures. This deviation can be partially attributed to the following:

Theory has assumed a spin of $S = \frac{1}{2}$ for the impurity while the Gd ion exhibits $S = \frac{7}{2}$. The use of a spin $S = \frac{1}{2}$ for Gd is justified, however, provided

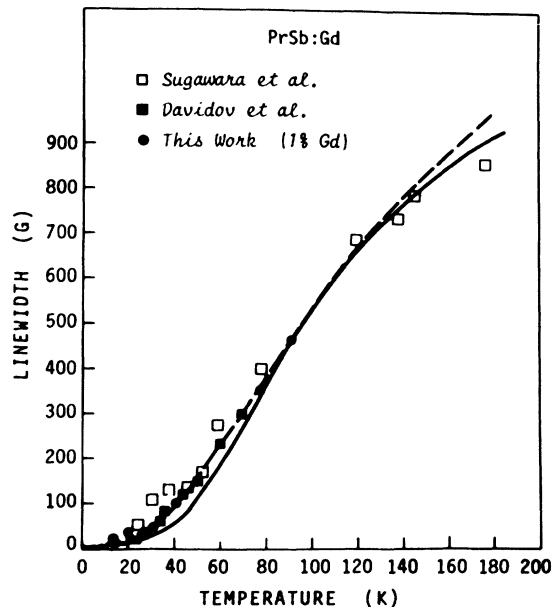


FIG. 9. Linewidth (after subtracting the residual width) of Gd in PrSb as a function of temperature. The solid line represents the fit of (16e) to the high-temperature experimental data. The fit of Sugawara *et al.* is given by the dashed line.

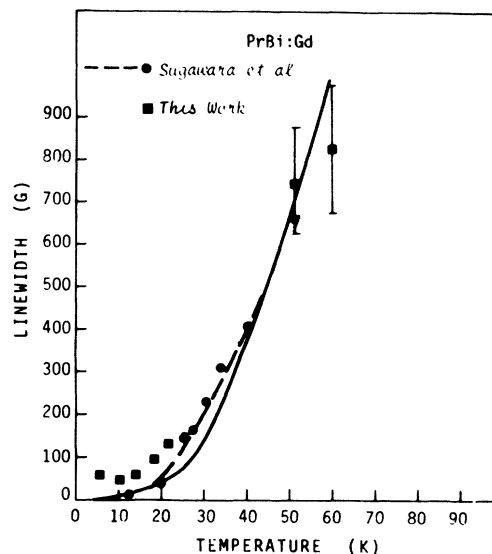


FIG. 10. Linewidth (after subtracting the residual width) of Gd in PrBi as a function of temperature. The solid line represents the fit of (16e) to the high-temperature experimental data. The fit of Sugawara *et al.* is given by the dashed line. The measurements were performed on a PrBi:Gd sample with 1.5% Gd and a residual width of 400 G was assumed.

that the Gd fine-structure lines are narrowed down to a single line^{6,34,35} (exchange narrowing collapse). This might not be the case for PrBi:Gd. The fine-structure splitting of Gd has been measured in several bismuthides^{36,37} (LaBi, YBi) and antimonides^{6,38,39} (LaSb, YSb, PrSb). It was found that the fourth-order crystalline-field parameter for Gd,¹³ b_4 , is very large in the bismuthides and smaller by a factor of 2, approximately, in the antimonides. The values of b_4 in the arsenides or the phosphides are also much smaller than it is in the heavier pnictides.⁴⁰ It is entirely possible, therefore, that for the case of PrBi:Bd, the fine-structure lines are not completely narrowed down at low temperatures even for Gd concentration in the vicinity of 1%.

The reason why the theory of Moriya and Obata agreed reasonably well with the experimental data, is probably due to the fact that the second moments are almost temperature independent in the higher-temperature regime (see Fig. 2). This is shown, however, for the first time in the present work. Furthermore, our theory enables us to extract the host exchange (but see below).

In the fitting procedure, we have used the crystalline-field energy levels as measured by others (Table III). This leaves us with a single parameter $(\mathcal{J}')^2/|\mathcal{J}|$ to be determined by fitting (16e) and (17) to the experimental linewidth. Table IV exhibits the various values of $(\mathcal{J}')^2/|\mathcal{J}|$ found by fitting the theory to experiment. The values of \mathcal{J}' were extracted previously^{4,6} from the ESR g shift of Gd in PrX ($X = \text{P, As, Sb, Bi}$). The values of $|\mathcal{J}|$ were estimated using the assumption that \mathcal{J}' is independent of the momentum transfer [i.e., $\langle(\mathcal{J}')^2\rangle = \langle\mathcal{J}'^2\rangle$]. These results as well as the values of

\mathcal{J}' are listed in Table IV. It is clearly seen that the magnitude of \mathcal{J} is larger than that of \mathcal{J}' . Also, there is a tendency of both \mathcal{J} and \mathcal{J}' to increase toward the heavy pnictides.

It is interesting to compare the values of $|\mathcal{J}|$ extracted from our ESR linewidth data with the values of \mathcal{J} estimated using combined susceptibility and neutron scattering results. The susceptibilities $\chi_m(0)$ of the various pnictides have been measured by several authors and are presented in Table IV. The value of χ_c in (34) can be calculated using the value of E_4 as measured by neutron scattering (Table III). The ratio of $\chi_m(0)$ and χ_c enables one to estimate J using (33). The results for the various pnictides are given in Table IV. Large differences (by an order of magnitude approximately) exist between the values of \mathcal{J} extracted by the different techniques. The NMR study of Myers and Narath, however, yielded a value of 0.053 meV for the exchange $|\mathcal{J}|$ in PrP (using their theory). This value is close to our value of $|\mathcal{J}| = 0.033$ meV in the same system (Table IV). In view of the different assumptions made in the ESR and NMR studies there is no real discrepancy between these two values. The discrepancy in Table IV, however, is not clearly understood at present. It can be partially attributed to the assumption made in our paper that both \mathcal{J} and \mathcal{J}' are independent of the momentum transfer \vec{q} . This assumption might be incorrect for metallic systems. In the presence of \vec{q} -dependent exchange interactions, the value of \mathcal{J} derived from susceptibility (or that derived from the ESR g shift) is actually the $\vec{q} = 0$ component of the exchange $\mathcal{J}(\vec{q} = 0)$, while that extracted from the ESR linewidth is $[\langle\mathcal{J}^2(q)\rangle]^{1/2}$. The difference might be significant.⁴¹ This possibility is un-

TABLE IV. A comparison between the exchange parameters extracted from ESR study and from susceptibility study.

Host	$(\mathcal{J}')^2/J^a$ (10^{-3} meV)	\mathcal{J}'^b (meV)	$ \mathcal{J} ^c$ (meV)	$\chi_m(0)^d$ (emu/mol)	χ_c^e (emu/mol)	\mathcal{J}^f (meV)
PrP	7.87	-0.016	0.033	0.034	0.025	+0.43
PrAs	6.23	-0.03	0.14	0.038	0.028	+0.43
PrSb	7.14	-0.08	0.896	0.052	0.044	+0.15
PrBi	28.95	-0.14	0.677	0.061	0.047	+0.20

^a Extracted by fitting (16e) and (17) to the experimental linewidth.

^b Derived from the Gd g shift (see Refs. 4 and 5) on the assumption of next-nearest-neighbor exchange only.

^c Extracted from the value of $(\mathcal{J}')^2/|\mathcal{J}|$ and \mathcal{J}' on the assumption of the Gaussian distribution (17).

^d Measured in Refs. (17) and (28).

^e Calculated from Eq. (35) using the values of E_4 in Table III.

^f Extracted from $\chi_m(0)$ and χ_c using (34).

likely, however, for PrP and PrAs. Finally, uncertainties in $\chi_m(0)$ as well as the approximate nature of (33) might also contribute to the disagreement between values of \mathcal{J} measured by the two methods.

IV. DISCUSSION

It is instructive to compare the linewidth behavior of Gd in PrIn_3 with the behavior observed in the Van Vleck pnictides. A unique feature of the $\text{PrIn}_3:\text{Gd}$ system is the very rapid thermal broadening of the ESR linewidth above 14 K (Fig. 4). This is unlike the behavior in the Van Vleck pnictides where a moderate increase of the linewidth was observed.

Let us discuss, first, the ESR properties of the pnictides. The results indicate^{4,5} that the initial decrease in the g shift and increase in the linewidth occur roughly at the same temperature. This might indicate that the same host crystal-field level is responsible for both these properties. We have demonstrated already⁶ [see also Eq. (31)] that the g shift reflects the admixture of the Γ_4 level with the singlet Γ_1 . We argue, therefore, that it is the Γ_4 level which is responsible for the *initial* thermal broadening. The level scheme, as measured by neutron scattering and shown in Table III, supports our interpretation. The Γ_4 level in the pnictides is always the lowest-lying excited state while the Γ_5 level is the highest level. This leads to a very small Γ_5 contribution to the Gd relaxation at low temperatures. We note, however, that the contribution of the Γ_5 level is significant already at a temperature of 50 K. This is because of the large oscillator strength associated with the transition within the Γ_5 levels, which is 25 times larger than that associated with the Γ_4 level [note the coefficients in front of the population factor in (16e)]. It is the small oscillator strength of the Γ_4 level which is responsible for the moderate increase of the linewidth versus temperature in the pnictides. The linewidth in the pnictides was interpreted using case *a*.

The situation is different in $\text{PrIn}_3:\text{Gd}$. In this system, we have observed the linewidth versus temperature to deviate significantly from linearity, at a temperature of approximately 14 K (Fig. 4). The g shift, however, is temperature independent up to 25 K. The temperature independence of the g shift, is consistent with the susceptibility study in Fig. 5 and according to (33). This might indicate that the g shift and the linewidth behavior above $T = 14$ K are associated with different crystalline-field levels of the host Pr ions: The g shift is due to admixture of the Γ_1 level with the Γ_4 level while the broadening phenomena can be ex-

plained by fluctuations within the Γ_5 multiplet. It is supported also by the following argument: The Γ_4 level in PrIn_3 is located at $E_4 = 105 \pm 10$ K. This value is comparable to or larger than the value of E_4 in the Pr pnictides. On the contrary, the Γ_5 level in PrIn_3 is lower in energy than in the pnictides. In view of the linewidth behavior in the pnictides, we do not expect, therefore, the rapid broadening in $\text{PrIn}_3:\text{Gd}$ to be associated with the Γ_4 level but with the Γ_5 level.⁴² The relatively low-lying Γ_5 level in PrIn_3 might indicate that case *c* is the dominant mechanism for relaxation in $\text{PrIn}_3:\text{Gd}$.

Recently, after this work was submitted for publication, we became aware that Knorr, Murani, and Gross⁴³ measured the crystalline-field splitting levels of Pr in PrIn_3 using inelastic neutron scattering technique. They found that Γ_1 is the ground state with Γ_4 as a first excited state at $E_4 = 100$ K. The Γ_5 level is located at $E_5 = 146$ K and the Γ_3 level is at $E_3 = 172$ K. These values are not inconsistent with the specific-heat study of Van Diepen *et al.*²⁶ and our susceptibility measurement. Adopting the values of Knorr, Murani, and Gross⁴³ one can calculate M_2 using (18) and $M_2(\Gamma_5)$ using (27). This enables us to calculate $1/T_2$ for case *a* and case *c* using (16e) and (28), respectively. The best fit of these two cases to the experimental linewidth is shown in Fig. 4. It is clearly seen that over the small temperature range available the fit is better with case *c*. This supports case *c* as the most likely mechanism for relaxation in PrIn_3 .

In conclusion, this paper presents new ESR data on the system $\text{PrIn}_3:\text{Gd}$ and analyzes the ESR relaxation of Gd in terms of a new theory for relaxation. The experimental results indicate that case *c* is most favorable for $\text{PrIn}_3:\text{Gd}$. We analyze also the ESR linewidth of Gd in Van Vleck pnictides, measured by others (and in the present work), in terms of case *a* of our theory. The fit of the theory to experiment enables one to extract the host exchange in the Van Vleck pnictides. Thus, ESR technique provides a powerful method for extracting the host exchange interaction. The importance of the data for $\text{PrIn}_3:\text{Gd}$ results from the fact that this is the first Van Vleck compound with relatively large conduction-electron density of states where relaxation phenomena associated with fluctuations of the host Pr ions have been observed.

ACKNOWLEDGMENTS

The authors wish to acknowledge E. Milosavljević for sample preparation and W. Wisny (FUB) for help in the susceptibility measurements.

APPENDIX A

The ESR relaxation of magnetic impurities in metallic Van Vleck compounds can be treated most generally by considering three coupled spin species: (a) the impurity spin S , (b) the spins of the host rare-earth ions (the Van Vleck ions), and (c) the spins of the conduction electrons. The calculation of the impurity ESR linewidth, therefore, must take into consideration the energy transfer between all three spin subsystems (as well as the lattice) in the presence of a static external magnetic field and a small transverse alternating field. One possible way to treat such a problem is to use a Hasegawa-like²⁹ equation of motion for the magnetization associated with the three spin subsystems.

In the present work, however, we shall assume that the conduction electrons and the host magnetic ions are in constant thermal equilibrium with the lattice²⁹ (nonbottleneck regime). In addition, we shall assume that the transverse susceptibility associated with the impurity at the impurity resonance frequency ω_0 is much larger than those of the other spin systems at the same frequencies ω_0 .

In this limit one can consider only the transverse magnetization M_x of the impurities and neglect the interaction between the rf field and the magnetic host ions as well as the conduction electrons. In other words, the magnetic host ions and the conduction electrons are "passive dissipative systems." The impurity ESR linewidth ΔH can be expressed in this approximation as

$$\Delta H = a + bT + \Delta H', \quad (\text{A1})$$

where a is the residual linewidth, b is the Korringa contribution originating with the impurity-conduction-electron exchange interaction given by Eq. (31), and $\Delta H'$ is the impurity linewidth due to the exchange interaction J' with the host paramagnetic ions [Eq. (6)].

The linewidth $\Delta H'$ can be calculated (under the assumptions above) starting with the following equation for the transverse component of the magnetization:

$$M_x = -\text{Tr} [g\mu_B S_x \sigma(t)], \quad (\text{A2})$$

where M_x and S_x are the x components of the impurity magnetization and spin, respectively, and $\sigma(t)$ is the density matrix for the impurity spin. Using Eq. (6) the kinetic equations for the density matrix $\sigma(t)$ can be obtained in analogy with those developed by many authors^{13,15,16,44} as

$$\frac{d\sigma_{mn}}{dt} = i[\sigma, \mathcal{H}_s + \mathcal{H}_s(t)]_{mn} + \sum_{k,l} R_{mnkl} \sigma_{kl}, \quad (\text{A3})$$

where the indices m, n, k, l represent the $2S+1$

different states of the impurity (with spin S) in the presence of an external magnetic field. (For a Gd impurity, $S = \frac{7}{2}$, these indices characterize the various crystalline-field levels in the presence of a magnetic field.) The Hamiltonian \mathcal{H}_s of the impurity includes the Zeeman interaction \mathcal{H}_Z , the crystalline-field interaction \mathcal{H}_{cf} , as well as first-order and second-order shifts (V_1 and V_2) of the g value (a general expression for \mathcal{H}_s is given at the end of this appendix). $\mathcal{H}_s(t)$ represents the interaction of the impurity spin with the alternating rf field, and R_{mnkl} are the Bloch-Redfield-Wangsness relaxation coefficients¹⁵ which may be represented in the form

$$R_{mnkl} = 2\Gamma_{mnkl} - \sum_j (\Gamma_{jnlj} \delta_{km} + \Gamma_{jkmj} \delta_{ln}), \quad (\text{A4})$$

with Γ_{mnkl} given [in the notation of Eq. (6)] as

$$\begin{aligned} \Gamma_{mnkl} &= \frac{\pi}{\hbar^2} [\mathcal{J}'(g_J - 1)]^2 \\ &\times \sum_{p,q=x,y,z} K'_{pq}(\omega_{ln}) \langle l | S_p | n \rangle \langle m | S_q | k \rangle, \end{aligned} \quad (\text{A5})$$

where $K'_{pq}(\omega_{ln})$ is the Fourier transform of the total correlation function defined as

$$K'_{pq}(\omega_{ln}) = \frac{1}{2\pi} \int_{-\infty}^{+\infty} e^{i\omega t} \left\langle \sum_{k=1}^{z_0} \delta J_p^{(k)}(t), \sum_{k=1}^{z_0} \delta J_q^{(k)} \right\rangle dt. \quad (\text{A6})$$

The fluctuation $\delta J_p^{(k)}$ of the angular momentum $J_p^{(k)}$ of the k th host rare-earth ion is defined by Eq. (10). In the absence of pair correlations in (A6) (i.e., absence of terms like $\langle \delta J_p^{(k)}, \delta J_q^{(j)} \rangle$ with $i \neq j$), Eq. (A6) is reduced to the form

$$K'_{pq}(\omega) = z_0 K_{pq}(\omega), \quad (\text{A7})$$

where now $K_{pq}(\omega)$ is defined by Eq. (8).

The resonance frequencies ω_{ln} in (A5) correspond to transitions between different l and n sublevels of the impurity S [$\omega_{ln} = (E_l - E_n)/\hbar$]. For the case where the inequality $|\omega_{mn} - \omega_{kl}| \gg R_{mnkl}$ is satisfied, the Eqs. (A3) can be further simplified. It has been demonstrated by Bloch¹⁵ and Hubbard¹⁵ that the condition $|\omega_{mn} - \omega_{kl}| \gg R_{mnkl}$ requires that only terms Γ_{mnkl} with $\omega_{mn} + \omega_{kl} = 0$ contribute to the expression (A4). Thus, in the case of nondegenerate and nonequidistant energy levels of the impurity spin (i.e., $\omega_{kl} \neq \omega_{mn}$ for $m \neq k$), the theory of Bloch^{13,15} yields

$$\frac{d\sigma_{mn}}{dt} = i[\sigma, \mathcal{H}_s + \mathcal{H}_s(t)]_{mn} - \frac{\sigma_{mn}}{T_{mn}}, \quad m \neq n$$

and

$$(\text{A8})$$

$$\frac{d\sigma_{mm}}{dt} = i[\sigma, \mathcal{H}_s + \mathcal{H}_s(t)]_{mm} + \sum_i (W_{im}\sigma_{ii} - W_{mi}\sigma_{mm}),$$

where $1/T_{mn}$ is the relaxation rate (equivalent to $1/T_2$) for the ESR line associated with the $m \rightarrow n$ transition between the m and n sublevels of the impurity. W_{mi} is related to the coefficients Γ in (A5) as

$$W_{mi} = 2\Gamma_{immi}. \quad (\text{A9})$$

Using (A8) it is easy to show¹⁶ that

$$\frac{1}{T_{mn}} = \frac{1}{2} \sum_k (W_{mk} + W_{nk}) - 2\Gamma_{mnmn} + \Gamma_{nnmm} + \Gamma_{mnmn}. \quad (\text{A10})$$

Equation (A10) can be applied to the relaxation rates of the various fine structure lines of Gd provided that the Gd fine-structure spectrum is completely resolved. This is indeed the case in Van Vleck pnictides at very low temperatures and small concentration.⁵ However, as the temperatures (or the Gd concentration) are increased, a collapse of the fine-structure lines into a single line occurs. The effect is very similar to that previously observed in LaSb:Gd.³⁶ In the extreme narrowed regime (A8) is no longer valid. For this regime, Zimmerman *et al.*³⁴ have demonstrated that the Gd relaxation rate can be described by kinetic equations with spin $S = \frac{1}{2}$ (rather than $S = \frac{7}{2}$). The problem solved by Zimmerman *et al.*³⁴ is very similar to the problem in the present work and one can use the approximation of $S = \frac{1}{2}$ to describe the Gd relaxation rate in the extreme narrowing regime. For $S = \frac{1}{2}$, Eqs. (A10), (A5), and (A7) yield Eq. (7) for cubic symmetry.

The various assumptions underlying Eqs. (A3) and (A4) can be summarized as follows^{15,16,44}:

(a) It is assumed that the relaxation coefficients R_{mnkl} are much smaller than the width $\Delta\omega$ of the

host fluctuation spectra. The width $\Delta\omega$ of the fluctuation spectra is of the order of the host exchange J . This has been shown by our moment calculations. The relaxation coefficients R_{mnkl} are of the order of the Gd experimental linewidth [see Eqs. (A4) and (A5)]. Thus, this condition is satisfied experimentally.

(b) The calculations have been done in the framework of the Born approximation, i.e., up to the second order in J .

(c) It was assumed that $\langle \mathcal{H}_s(t) \rangle_{\max} \tau_c \ll 1$. Here τ_c is related to $\Delta\omega$ as $\Delta\omega \cong 1/\tau_c$. This condition was certainly met in our experiments.

Finally, we shall give an expression for \mathcal{H}_s in (A3). \mathcal{H}_s can be expressed as

$$\mathcal{H}_s = \mathcal{H}_{cf} + \mathcal{H}_Z + V_1 + V_2,$$

where V_1 is the first-order shift, and V_2 is the second-order shift given by⁴⁴

$$V_1 = \text{Tr}_{\{J\}} [\mathcal{H}'_{ex} \rho(\mathcal{H})],$$

where \mathcal{H}'_{ex} is the exchange interaction Eq. (6), $\rho(\mathcal{H})$ is the Gibbs distribution function of the host, and the index $\{J\}$ indicates that the trace is taken over the host quantum numbers only. The value of V_2 is given by^{44,45}

$$V_2 = \sum_{p,q} \sum_{m,n,m'} \left(P \int_{-\infty}^{\infty} \frac{K_{pq}(\omega)}{\omega_{mn} - \omega} d\omega \right) P_m S_p P_n S_q P_{m'},$$

where $P \int_{-\infty}^{\infty}$ denotes the principle part of the integral, $K_{pq}(\omega)$ is from Eq. (A6) and P_m, P_n are the projection operators for the impurity states.

APPENDIX B: CALCULATION OF THE SECOND MOMENT M_2 OF $F(\omega)$

The second moment of the spectral function $K_{zz}(\omega)$ is defined as

$$\left(\int_{-\infty}^{\infty} K_{zz}(\omega) \omega^2 d\omega \right) \left(\int_{-\infty}^{\infty} K_{zz}(\omega) d\omega \right)^{-1} = \frac{-\text{Tr} \{ \rho(\mathcal{H}) [\mathcal{H}, J_z^{(1)}]_I^2 \}}{\text{Tr} [\rho(\mathcal{H}) (J_z^{(1)})^2]}, \quad (\text{B1})$$

where $\rho(\mathcal{H})$ is the Gibbs function and the Hamiltonian \mathcal{H} is given by the sum of the exchange Hamiltonian (4) and the crystalline-field Hamiltonian (3). The second moment (B1) does not represent the second moment of $F(\omega)$. This is because (B1) also contains contributions originating with the high-frequency components of $K_{zz}(\omega)$. It is necessary, therefore, to apply a truncation procedure to the operators $J_z^{(1)}$ and \mathcal{H}_{ex} , responsible for the broadening. This truncation is obtained by taking the secular part of \mathcal{H}_{ex} and only those matrix elements of $J_z^{(1)}$ which contribute to the low-frequency part of the fluctuation spectra. Using (B1) together with the truncated operators and the approximation $\rho(\mathcal{H}) = \rho(\mathcal{H}_{cf})$, the second moment M_2 of $F(\omega)$ can be written

$$M_2 = \left(\int_{-\infty}^{+\infty} K_{zz}^{\text{LF}}(\omega) \omega^2 d\omega \right) \left(\int_{-\infty}^{+\infty} K_{zz}^{\text{LF}}(\omega) d\omega \right)^{-1} = \frac{-\text{Tr} \{ \rho(\mathcal{H}_{cf}) [\overline{\mathcal{H}}_{ex}, \overline{J}_z^{(1)}]_I^2 \}}{\text{Tr} [\rho(\mathcal{H}_{cf}) (\overline{J}_z^{(1)})^2]}, \quad (\text{B2})$$

where the bars mean truncated operators satisfying

$$[\bar{\mathcal{C}}_{\text{ex}}, \mathcal{C}_{\text{cf}}] = 0, \quad [\bar{J}_z^{(1)}, \mathcal{C}_{\text{cf}}] = 0. \quad (\text{B3})$$

In order to calculate the traces in (B2) we define a complete set of functions

$$|n, f_n\rangle = \prod_{i=1}^N |\Gamma_\alpha, f_\alpha\rangle_i, \quad (\text{B4})$$

where $|\Gamma_\alpha, f_\alpha\rangle_i$ are the eigenfunctions of the "single-ion" crystalline-field operator (3) and the index i runs over the N Pr ions. The index n specifies the total energy

$$E_n \left(E_n = \sum_{i=1}^N E_\alpha \right)$$

and f specifies various wave functions correspond-

ing to a given energy E_n . This degeneracy arises from the degeneracy with the "single-ion" spectrum as well as from different permutations of the "single-ion" wave functions in (B4).

We then introduce the projection operators P_{nf_n} with the property

$$P_{nf_n} |n', f'_n\rangle = \delta_{nn'} \delta_{ff'} |n, f_n\rangle, \quad (\text{B5})$$

with the help of these projection operators the truncated operators $\bar{\mathcal{C}}_{\text{ex}}$ and $\bar{J}_z^{(1)}$ can be expressed as

$$\bar{\mathcal{C}}_{\text{ex}} = \sum_{f_n, f'_n} P_{nf_n} \mathcal{C}_{\text{ex}} P_{nf'_n}, \quad (\text{B6})$$

$$\bar{J}_z^{(1)} = \sum_{n, f_n} P_{nf_n} J_z^{(1)} P_{nf_n}. \quad (\text{B7})$$

Inserting (B6) and (B7) in (B2) yields

$$\text{Tr}[\rho(\mathcal{C}_{\text{cf}})(\bar{J}_z^{(1)})^2] = \sum_\alpha p_\alpha |\langle \Gamma_\alpha f_\alpha | J_z^{(1)} | \Gamma_\alpha f_\alpha \rangle|^2,$$

$$\begin{aligned} -\text{Tr}\{\rho(\mathcal{C}_{\text{cf}})[\bar{\mathcal{C}}_{\text{ex}}, \bar{J}_z^{(1)}]^2\} = Z^{-2} \sum_{i \neq 1} \sum_{\substack{\alpha, \beta, f_\alpha, f_\beta \\ f'_\alpha, f'_\beta}} e^{-(E_\alpha + E_\beta)/T} \times [& |\langle \Gamma_\alpha f_\alpha, \Gamma_\beta f_\beta | \mathcal{C}_{\text{ex}}^{(1,i)} | \Gamma_\alpha f'_\alpha, \Gamma_\beta f'_\beta \rangle|^2 \\ & \times (\langle \Gamma_\alpha f'_\alpha | J_z^{(1)} | \Gamma_\alpha f'_\alpha \rangle - \langle \Gamma_\alpha f_\alpha | J_z^{(1)} | \Gamma_\alpha f_\alpha \rangle)^2 \\ & + (1 - \delta_{\alpha\beta}) |\langle \Gamma_\alpha f_\alpha, \Gamma_\beta f_\beta | \mathcal{C}_{\text{ex}}^{(1,i)} | \Gamma_\beta f'_\beta, \Gamma_\alpha f'_\alpha \rangle|^2 \\ & \times (\langle \Gamma_\beta f'_\beta | J_z^{(1)} | \Gamma_\beta f'_\beta \rangle - \langle \Gamma_\alpha f_\alpha | J_z^{(1)} | \Gamma_\alpha f_\alpha \rangle)^2], \end{aligned} \quad (\text{B8})$$

where $\mathcal{C}_{\text{ex}}^{(1i)}$ is the exchange interaction between the ion labeled "1" and the i th ion. The wave function $\langle \Gamma_\alpha f_\alpha, \Gamma_\beta f_\beta |$ represents a "two-ion" wave function where the first two indices characterize the ion labeled "1" and the last two indices characterize the wave function appropriate to the i th ion. We have omitted in (B8) terms which contain sums of the form

$$\sum_{i \neq 1'} \mathcal{C}_{\text{ex}}^{(1i)} \mathcal{C}_{\text{ex}}^{(1i')}.$$

These terms are zero for *isotropic* exchange interactions and diagonal J_z operators within each multiplet. It is easy to extend our calculations to include the anisotropic exchange interaction. For the singlet-ground-state system of Pr compounds (B7) and (B8) yield for M_2 the expression given by (18).

APPENDIX C: CALCULATION OF THE FOURTH MOMENT M_4 OF $F(\omega)$

In analogy with Appendix B, the fourth moment of the low-frequency part of $K_{zz}(\omega)$ can be expressed as

$$M_4 = \frac{\text{Tr}\{\rho(\mathcal{C}_{\text{cf}})[\bar{\mathcal{C}}, [\bar{\mathcal{C}}, \bar{J}_z^{(1)}]]\}}{\text{Tr}[\rho(\mathcal{C}_{\text{cf}})(J_z^{(1)})^2]}, \quad (\text{C1})$$

where, again, $\bar{\mathcal{C}} = \mathcal{C}_{\text{cf}} + \bar{\mathcal{C}}_{\text{ex}}$ and the bars mean truncated operators defined by (B4) and (B5). The denominator of (C1) can be expressed as

$$\text{Tr}[\rho(\mathcal{C}_{\text{cf}})(J_z^{(1)})^2] = \sum_\alpha p_\alpha |\langle \Gamma_\alpha f_\alpha | J_z^{(1)} | \Gamma_\alpha f_\alpha \rangle|^2.$$

The numerator of (C1) can be expressed as

$$\begin{aligned}
& \text{Tr}\{\rho(\mathcal{H}_{\text{eff}})[\overline{\mathcal{H}}, [\overline{\mathcal{H}}, \overline{J}_x^{(1)}]]\} \\
&= Z^{-2} \sum_{i \neq 1} \sum_{\substack{\Gamma_\alpha f_\alpha \\ \Gamma_\beta f_\beta \\ f'_\alpha f'_\beta}} e^{-(E_\alpha + E_\beta)/T} \left[\left(\sum_{f''_\alpha f''_\beta} \langle \Gamma_\alpha f_\alpha, \Gamma_\beta f_\beta | \mathcal{H}_{\text{ex}}^{(i,1)} | \Gamma_\alpha f''_\alpha \Gamma_\beta f''_\beta \rangle \langle \Gamma_\alpha f''_\alpha \Gamma_\beta f''_\beta | \mathcal{H}_{\text{ex}}^{(i,1)} | \Gamma_\alpha f'_\alpha \Gamma_\beta f'_\beta \rangle \right. \right. \\
&\quad \times \left(\langle \Gamma_\beta f'_\beta | J_z^{(1)} | \Gamma_\beta f'_\beta \rangle - 2 \langle \Gamma_\beta f'_\beta | J_z^{(1)} | \Gamma_\beta f''_\beta \rangle + \langle \Gamma_\beta f'_\beta | J_z^{(1)} | \Gamma_\beta f_\beta \rangle \right) \\
&\quad + (1 - \delta_{\alpha\beta}) \sum_{f''_\alpha f''_\beta} \langle \Gamma_\alpha f_\alpha \Gamma_\beta f_\beta | \mathcal{H}_{\text{ex}}^{(i,1)} | \Gamma_\beta f''_\alpha \Gamma_\alpha f''_\beta \rangle \langle \Gamma_\beta f''_\alpha \Gamma_\alpha f''_\beta | \mathcal{H}_{\text{ex}}^{(i,1)} | \Gamma_\alpha f'_\alpha \Gamma_\beta f'_\beta \rangle \\
&\quad \times \left(\langle \Gamma_\beta f'_\beta | J_z^{(1)} | \Gamma_\beta f'_\beta \rangle - 2 \langle \Gamma_\alpha f''_\alpha | J_z^{(1)} | \Gamma_\alpha f''_\alpha \rangle + \langle \Gamma_\beta f_\beta | J_z^{(1)} | \Gamma_\beta f_\beta \rangle \right) \Big)^2 \\
&\quad + (1 - \delta_{\alpha\beta}) \left(\sum_{f''_\alpha f''_\beta} \langle \Gamma_\alpha f_\alpha \Gamma_\beta f_\beta | \mathcal{H}_{\text{ex}}^{(i,1)} | \Gamma_\alpha f''_\alpha \Gamma_\beta f''_\beta \rangle \langle \Gamma_\alpha f''_\alpha \Gamma_\beta f''_\beta | \mathcal{H}_{\text{ex}}^{(i,1)} | \Gamma_\beta f'_\beta \Gamma_\alpha f'_\alpha \rangle \right. \\
&\quad \times \left(\langle \Gamma_\alpha f'_\alpha | J_z^{(1)} | \Gamma_\alpha f'_\alpha \rangle - 2 \langle \Gamma_\beta f''_\beta | J_z^{(1)} | \Gamma_\beta f''_\beta \rangle + \langle \Gamma_\beta f_\beta | J_z^{(1)} | \Gamma_\beta f_\beta \rangle \right) \\
&\quad + \sum_{f''_\alpha f''_\beta} \langle \Gamma_\alpha f_\alpha \Gamma_\beta f_\beta | \mathcal{H}_{\text{ex}}^{(i,1)} | \Gamma_\beta f''_\beta \Gamma_\alpha f''_\alpha \rangle \langle \Gamma_\beta f''_\beta \Gamma_\alpha f''_\alpha | \mathcal{H}_{\text{ex}}^{(i,1)} | \Gamma_\beta f'_\beta \Gamma_\alpha f'_\alpha \rangle \\
&\quad \times \left(\langle \Gamma_\alpha f'_\alpha | J_z^{(1)} | \Gamma_\alpha f'_\alpha \rangle - 2 \langle \Gamma_\alpha f''_\alpha | J_z^{(1)} | \Gamma_\alpha f''_\alpha \rangle \right. \\
&\quad \left. \left. + \langle \Gamma_\beta f_\beta | J_z^{(1)} | \Gamma_\beta f_\beta \rangle \right) \right] + \dots, \tag{C2}
\end{aligned}$$

where the dots stand for terms originating with “three particle” and “four particle” processes, where the wave functions $\langle \Gamma_\alpha f_\alpha, \Gamma_\beta f_\beta |$ are already defined in Appendix B. The denominators of (B1) have been calculated in a way similar to that in Appendix B. We have retained in (B2) only those terms originating with “two-ion” processes. Similar terms have been observed for “three-ion” and “four-ion” processes but have not been expressed explicitly in (C2) for simplicity. In the limit of $T=0$ the fourth moment M_4 has been calculated explicitly using (C1), (C2), and (B8). Its expression for the case of $J=4$ (Pr^{+3}) is given by (20), in this limit. The temperature dependence of the fourth moment can be computed and will be published elsewhere.

APPENDIX D: CALCULATIONS OF THE SECOND MOMENTS $M_2(\Gamma_4)$ AND $M_2(\Gamma_5)$ OF THE SPECTRAL FUNCTIONS $F_1(\omega - \omega_{44})$ AND $F_2(\omega - \omega_{55})$

The second moments in this case are defined as

$$M_2(\Gamma_4) = \int_{-\infty}^{+\infty} (\omega - \omega_{44})^2 F_1(\omega - \omega_{44}) d\omega, \tag{D1}$$

$$M_2(\Gamma_5) = \int_{-\infty}^{+\infty} (\omega - \omega_{55})^2 F_2(\omega - \omega_{55}) d\omega. \tag{D2}$$

In calculating $M_2(\Gamma_4)$ and $M_2(\Gamma_5)$, we start with the second moment of $K_{xx}(\omega)$ and use the projection-operator technique. We define a truncation operator $\overline{J}_x^{(1)}$ given by

$$\overline{J}_x^{(1)} = \sum_{n, f_n} P_{n f_n} J_x^{(1)} P_{n' f_{n'}}. \tag{D3}$$

The projection operators P are chosen such that

$$E_{n f_n} - E_{n' f_{n'}} = g_\alpha \beta H \quad (\alpha = 4, 5), \tag{D4}$$

with the values of g_α defined by (15). The relation (D4) guarantees that only matrix elements of $J_x^{(1)}$ between $|\Gamma_\alpha f_\alpha\rangle$ ($\alpha = 4, 5$) of the multiplet Γ_α will contribute to the second moment. Our calculations were carried out in the same manner as described in Appendix B. The results are given by Eqs. (26) and (27).

*Supported by the U.S.—Israel Binational Science Foundation; also supported in part by the Deutsche-Forschungsgemeinschaft SFB 161.

†Also at Fachbereich Physik, Freie Universität, Berlin, West Germany.

¹Y. L. Wang and B. R. Cooper, Phys. Rev. **172**, 539 (1968); **185**, 696 (1969); B. R. Cooper, Phys. Rev. B **6**, 2730 (1972); Y. Hsieh and M. Blume, *ibid.* **6**, 2708 (1972); M. Blume and R. J. Birgeneau, J. Phys. C **7**, L282 (1974); for earlier works see G. T. Trammel, J. Appl. Phys. **31**, 3625 (1960); G. T. Trammel, Phys.

Rev. **131**, 932 (1963); B. Bleaney, Proc. R. Soc. A **276**, 19 (1963); R. N. Bozorth and J. H. Van Vleck, Phys. Rev. **118**, 1493 (1960); B. Grover, *ibid.* **140**, A1944 (1965).

²Y. L. Wang and B. R. Cooper, Phys. Rev. **172**, 539 (1968); **185**, 696 (1969).

³R. J. Birgeneau, J. Als-Nielsen, and E. Bucher, Phys. Rev. Lett. **27**, 1530 (1971); Phys. Rev. B **6**, 2724 (1972); B. R. Cooper, *ibid.* **6**, 2730 (1972).

⁴K. Sugawara, C. Y. Huang, and B. R. Cooper, Phys. Rev. B **11**, 4455 (1975).

- ⁵C. Rettori, D. Davidov, A. Gragevsky, and W. M. Walsh, *Phys. Rev. B* **11**, 4450 (1975).
- ⁶D. Davidov, C. Rettori, and V. Zevin, *Solid State Commun.* **16**, 247 (1975).
- ⁷D. Davidov and K. Baberschke, *Phys. Lett. A* **51**, 144 (1975).
- ⁸C. Rettori, R. Levin, and D. Davidov, *J. Phys. F* (to be published).
- ⁹The ESR resonance originating from Dy^{+3} and Yb^{+3} in PrSb and TmSb have been observed by C. Rettori, D. Davidov, and K. Baberschke (unpublished).
- ¹⁰B. R. Cooper and O. Vogt, *J. Phys. (Paris)* **32**, C1-958 (1971).
- ¹¹R. J. Birgeneau, *AIP Conf. Proc.* **10**, 1664 (1972).
- ¹²The resonance properties of $PrIn_3:Gd$ at low temperatures ($1.4 \leq T \leq 4.2$ K) were determined separately by C. Rettori and D. Davidov (unpublished).
- ¹³C. P. Slichter, in *Principle of Magnetic Resonance*, edited by F. Seitz (Harper, New York, 1963); A. Abragam, in *Principles of Nuclear Magnetism* (Oxford U.P., New York, 1961).
- ¹⁴T. Moriya and Y. Obata, *J. Phys. Soc. Jpn.* **13**, 1333 (1958).
- ¹⁵F. Bloch and P. Wangsness, *Phys. Rev.* **89**, 728 (1953); F. Bloch, *ibid.* **102**, 104 (1956); A. Redfield, *ibid.* **98**, 1787 (1955); P. Hubbard, *Rev. Mod. Phys.* **33**, 249 (1961).
- ¹⁶V. M. Fain, *Zh. Eksp. Teor. Fiz.* **42**, 1075 (1962) [*Sov. Phys.-JETP* **15**, 743 (1962)].
- ¹⁷R. P. Guertin, J. E. Crow, L. D. Longinotti, E. Bucher, L. Kupferberg, and S. Foner, *Phys. Rev. B* **12**, 1005 (1975).
- ¹⁸K. C. Turberfield, L. Passell, R. J. Birgeneau, and E. Bucher, *Phys. Rev. Lett.* **25**, 752 (1970); *J. Appl. Phys.* **42**, 1746 (1971).
- ¹⁹A. Abragam and B. Bleaney, *Electron Paramagnetic Resonance of Transition Ions* (Oxford U.P., London, 1970).
- ²⁰M. T. Hutchings, in *Solid State Physics*, edited by F. Seitz, D. Turnbull, and H. Ehrenreich (Academic, New York, 1964), Vol. 16.
- ²¹K. R. Lea, M. J. M. Leask, and W. P. Wolf, *J. Phys. Chem. Solids* **23**, 1381 (1962).
- ²²M. McMillan and W. Opechowski, *Can. J. Phys.* **38**, 2915 (1963).
- ²³M. H. L. Pryce and K. W. H. Stevens, *Proc. Phys. Soc. Lond. A* **63**, 36 (1951).
- ²⁴V. Zevin and B. Shanina, *Ukr. Fiz. Zh.* **11**, 1089 (1966).
- ²⁵S. M. Myers and A. Narath, *Phys. Rev. B* **9**, 227 (1974).
- ²⁶A. M. Van Diepen, R. S. Craig, and W. E. Wallace, *J. Phys. Chem. Solids* **32**, 1867 (1971).
- ²⁷E. Bucher, K. Andres, A. C. Gossard, and J. P. Maita, *Low Temp. Conf. Proc.* **2**, 332 (1974).
- ²⁸E. Bucher, K. Andres, J. P. Maita, A. S. Cooper, and L. D. Longinotti, *J. Phys. (Paris)* C1-115 (1970).
- ²⁹H. Hasegawa, *Prog. Theor. Phys.* **21**, 483 (1959); D. Davidov, A. Chelkowski, C. Rettori, R. Orbach, and M. B. Maple, *Phys. Rev. B* **7**, 1029 (1972).
- ³⁰L. B. Welsh, C. L. Wiley, and F. Fradin, *Phys. Rev. B* **11**, 4156 (1975).
- ³¹E. Bucher, J. P. Maita, and A. S. Cooper, *Phys. Rev. B* **6**, 2709 (1972).
- ³²G. Fehr and A. F. Kip, *Phys. Rev.* **98**, 377 (1955); F. J. Dyson, *ibid.* **98**, 349 (1955).
- ³³M. Peter, D. Shaltiel, J. H. Wernick, H. J. Williams, J. B. Mock, and R. C. Sherwood, *Phys. Rev.* **126**, 1395 (1962).
- ³⁴P. H. Zimmermann, D. Davidov, R. Orbach, L. J. Tao, and J. Zitkova, *Phys. Rev. B* **6**, 2783 (1972).
- ³⁵P. Urban, D. Davidov, B. Elschner, T. Plefka, and G. Sperlich, *Phys. Rev. B* **12**, 72 (1975).
- ³⁶P. Urban, B. Elschner, G. Sperlich, and G. Schon, *Phys. Lett. A* **49**, 418 (1974).
- ³⁷K. Baberschke, D. Davidov, C. Rettori, *Low Temp. Conf. Proc.* **3**, 484 (1975).
- ³⁸D. Davidov, C. Rettori, G. Ng, and E. P. Chock, *Phys. Lett. A* **49**, 320 (1974).
- ³⁹D. Davidov, C. Rettori, and D. Shaltiel, *Phys. Lett. A* **50**, 393 (1974).
- ⁴⁰G. Sperlich and P. Urban (private communication).
- ⁴¹The assumption of the independence of the exchange parameters on momentum transfer can be dangerous for the case of the heavy pnictides PrSb and PrBi. The value of J estimated for the heavy pnictides on the basis of this assumption are very large, violating the requirement (1) necessary for a weakly coupled Van Vleck.
- ⁴²We note that the exchange interaction between the Gd and the host Pr ions is larger in $PrIn_3:Gd$ with respect to that in the light pnictides but is of the same order of magnitude as in $PrBi:Gd$. Thus, the larger value of J' in $PrIn_3:Gd$ cannot explain the larger relaxation rate in this system.
- ⁴³K. Knorr, A. Murani, W. Gross, and K. H. J. Buschow (private communication).
- ⁴⁴P. Argyers and K. Kelley, *Phys. Rev.* **134**, A48 (1964).
- ⁴⁵B. Shanina, Ph.D. thesis (unpublished).